

1 **Limited population structure but signals of recent selection in introduced African Fig** 2 **Fly (*Zaprionus indianus*) in North America**

3
4 Priscilla A. Erickson^{1*}, Alyssa Bangerter², Ansleigh Gunter¹, Nikolaos T. Polizos³, and Alan O.
5 Bergland²

- 6
7 1. University of Richmond, Richmond, Virginia
8 2. University of Virginia, Charlottesville, Virginia
9 3. University of Miami, Coral Gables, Florida

10 *Corresponding author; perickso@richmond.edu

11 12 **Running title**

13
14 Genomics of invasive *Zaprionus indianus*

15 16 **Abstract**

17
18 Invasive species have devastating consequences for human health, food security, and the
19 environment. Many invasive species adapt to new ecological niches following invasion, but
20 little is known about the early steps of adaptation. Here we examine population genomics of a
21 recently introduced drosophilid in North America, the African Fig Fly, *Zaprionus indianus*. This
22 species is likely intolerant of subfreezing temperatures and recolonizes temperate
23 environments yearly. We generated a new chromosome-level genome assembly for *Z.*
24 *indianus*. Using resequencing of over 200 North American individuals collected over four years
25 in temperate Virginia, plus a single collection from subtropical Florida, we tested for signatures
26 of recolonization, population structure, and adaptation within invasive populations. We show
27 founding populations are sometimes small and contain close genetic relatives, yet temporal
28 population structure and differentiation of populations is mostly absent across recurrent
29 recolonization events. Although we find limited signals of genome-wide spatial or temporal
30 population structure, we identify haplotypes on the X chromosome that are repeatedly
31 differentiated between Virginia and Florida populations. These haplotypes show signatures of
32 natural selection and are not found in African populations. We also find evidence for several
33 large structural polymorphisms segregating within North America populations and show X
34 chromosome evolution in invasive populations is strikingly different from the autosomes. These
35 results show that despite limited population structure, populations may rapidly evolve genetic
36 differences early in an invasion. Further uncovering how these genomic regions influence
37 invasive potential and success in new environments will advance our understanding of how
38 organisms evolve in changing environments.

39 40 **Article Summary**

41
42 Invasive species (organisms that have been moved outside their natural range by human
43 activities) can cause problems for both humans and the environment. We studied the genomes

44 of over 200 individuals of a newly invasive fruit fly in North America, the African Fig Fly. We
45 found genetic evidence that these recently introduced flies may be evolving in their new
46 environments, which could make them stronger competitors and more likely to become pests.

47

48 **Introduction**

49

50 Understanding how species expand and adapt to new environments in an era of climate
51 change and global commerce is central to controlling the spread of disease (Altizer et al. 2013;
52 Hoberg and Brooks 2015), to maintaining crop security (Oerke 2006; Sutherst et al. 2011) and
53 to preserving biodiversity (Bellard et al. 2012). Many organisms are moving to new, previously
54 unoccupied ranges at rates that continue to accelerate (Ricciardi 2007; Seebens et al. 2015;
55 Seebens et al. 2017; Platts et al. 2019; Sardain et al. 2019) due to changes in climate and
56 habitat as well as anthropogenic introductions. Genetic adaptation to new environments may
57 allow some vulnerable organisms to survive in new habitats but may also permit potentially
58 harmful organisms to expand even further (Clements and Ditommaso 2011). The past two
59 decades have produced a wealth of studies characterizing the genetic and genomic basis of
60 adaptation in a variety of organisms, from experimental populations of microbes (Good et al.
61 2017; Nguyen Ba et al. 2019; Johnson et al. 2021) to natural populations of eukaryotes
62 (Hancock et al. 2011; Jones et al. 2018; Barrett et al. 2019; Lovell et al. 2021; Schluter et al.
63 2021). Recent and ongoing invasions offer the opportunity to study rapid evolution and
64 adaptation to new environments in nearly real-time (Koch et al. 2020; Pélissié et al. 2022;
65 Parvizi et al. 2023; Soudi et al. 2023). Recently, genomics has helped trace the history and
66 sources of many well-known invasions (Pélissié et al. 2022; Picq et al. 2023) and shown that
67 genetic divergence and even local adaptation are common in invasive populations that have
68 been established for decades or even centuries (Ma et al. 2020; Stuart et al. 2021; Li et al.
69 2023). However, much remains unknown about the genetic mechanisms that allow invasive
70 organisms to colonize and thrive in new environments. A better understanding of adaptive
71 pathways in invasion may assist in predicting the success of invasions and controlling their
72 outcomes.

73

74 The African Fig Fly, *Zaprionus indianus*, serves as a unique model to study how
75 invasion history and local environment influence patterns of genetic variation. The ongoing,
76 recurrent invasion of *Z. indianus* in North America offers a premier opportunity to study the
77 possibility of rapid genetic changes following invasion. The *Zaprionus* genus arose in Africa but
78 *Z. indianus* was first described in India in 1970 (Gupta 1970), where it has adapted to a range
79 of environments (da Mata et al. 2010). It is one of the most ecologically diverse drosophilids in
80 Africa; its ability to utilize up to 80 different food sources (Yassin and David 2010) and its
81 generation time of as few as ~13 days (Nava et al. 2007) likely fueled its spread around the
82 world. In 1999, it was first detected in Brazil (Vilela 1999), where it subsequently spread and
83 caused major damage to fig and berry crops as well as native fruit species (Leão and Tidon
84 2004; Oliveira et al. 2013; Roque et al. 2017; Zanuncio-Junior et al. 2018; Allori Stazzonelli et
85 al. 2023). It was later found in Mexico and Central America in 2002-2003 (Markow et al. 2014)
86 and eventually Florida in 2005 (Linde et al. 2006). In 2011-2012, its range expanded

87 northwards in eastern North America (Joshi et al. 2014; Timmeren and Isaacs 2014; Pfeiffer et
88 al. 2019) and eventually reached as far north as Ontario (Renkema et al. 2013) and Minnesota
89 (Holle et al. 2018). It has also recently been found in the Middle East, Europe, and Hawaii
90 (Parchami-Araghi et al. 2015; Kremmer et al. 2017; Willbrand et al. 2018), suggesting that the
91 invasion is ongoing. *Z. indianus* can damage fig and berry crops (Pfeiffer et al. 2019; Allori
92 Stazzonelli et al. 2023), increasing concerns about its pest potential in its expanding range.

93
94 Despite its global success, *Z. indianus* males are sterile below 15 °C, making cold
95 temperatures a limiting factor to their success (Araripe et al. 2004). Within the temperate
96 environment of Virginia, the species exhibits strong seasonal fluctuations in abundance (Rakes
97 et al. 2023). First detection in Virginia is usually in June or July, weeks after the appearance of
98 other overwintering Drosophilids, and population sizes climb dramatically through the late
99 summer and early fall, when it often dominates the drosophilid community in temperate
100 orchards. Typically, the peak in early to mid-September is followed by a dip in abundance and
101 then a second peak in October, suggesting a seasonal component to reproduction or
102 fluctuations in factors influencing *Z. indianus*' relative fitness. However, despite its early post-
103 colonization success, it does not appear to survive temperate winters; *Z. indianus* populations
104 became undetectable in Virginia by early December (Rakes et al. 2023). In locations in
105 Minnesota, Kansas, and the northeastern US, *Z. indianus* has been detected one year and
106 then not the next, suggesting that the populations are not permanently established, but are
107 extirpated by cold and re-introduced by stochastic dispersal processes (Holle et al. 2018;
108 Gleason et al. 2019; Rakes et al. 2023). Therefore, *Z. indianus* likely repeatedly invades
109 temperate environments and evolves for several generations in these new habitats, offering an
110 opportunity to recurrently study the genetic impacts of invasion and post-colonization
111 adaptation across multiple years of sampling.

112
113 Genetic studies of *Z. indianus* are limited but provide important context to understand its
114 worldwide invasion. The invasion of North America likely resulted from separate founding
115 events on the East and West coasts (Commar et al. 2012). Comeault *et al* (2020) showed that
116 North American populations are genetically distinct from those from Africa. Invasive
117 populations of *Z. indianus* have an approximately 30% reduction in genetic diversity relative to
118 ancestral African populations (Comeault et al. 2020), though invasive populations of *Z.*
119 *indianus* maintain levels of genetic diversity that are often higher than those of non-invasive
120 congeners. Despite the loss of diversity, *Z. indianus* is extremely successful in temperate
121 habitats (Rakes et al. 2023). Further studies demonstrated that genetically distinct populations
122 from eastern and western Africa likely admixed prior to a single colonization of the Americas
123 (Comeault et al. 2021). How the high degree of genetic diversity in invasive populations
124 influences the potential for ongoing evolution in North America, which is in a critical early stage
125 of invasion, remains understudied.

126
127 Here, we assembled and annotated a chromosome-level genome assembly for *Z.*
128 *indianus* and used the newly improved genome to answer several questions with the whole
129 genome sequences of over 200 North American flies collected from three locations over four

130 years. First, do recolonizing North American *Z. indianus* populations demonstrate spatial or
131 temporal population structure and if so, do specific regions of the genome have an outsized
132 contribution to population structure? Second, is the invasion and recolonization history
133 recapitulated in population genetic data? And third, do temperate populations show signatures
134 of selection relative to native and tropical invasive populations?

135

136 **Materials and Methods**

137

138 *Hi-C based genome scaffolding*

139

140 An inbred line was generated from flies originally captured from Carter Mountain Orchard, VA
141 (37.9913° N, 78.4721° W) in 2018. Wild caught flies were reared in the lab for approximately
142 one year prior to initiating isofemale lines. The offspring of the isofemale lines were propagated
143 through 10 rounds of full-sib mating. The resulting lines were then passaged for approximately
144 one additional year in the lab and the most vigorous remaining line (“24.2”) was chosen for
145 sequencing.

146

147 3rd instar larvae from a single inbred line were snap frozen in liquid nitrogen and sent to
148 Dovetail corporation (now Cantata Bio, Scotts Valley, CA) for chromatin extraction, Hi-C
149 sequencing and genome scaffolding. Briefly, chromatin was fixed in place with formaldehyde in
150 the nucleus and then extracted. Fixed chromatin was digested with DNase I, chromatin ends
151 were repaired and ligated to a biotinylated bridge adapter followed by proximity ligation of
152 adapter containing ends. After proximity ligation, crosslinks were reversed and the DNA
153 purified. Purified DNA was treated to remove biotin that was not internal to ligated fragments.
154 Sequencing libraries were generated using NEBNext Ultra enzymes and Illumina-compatible
155 adapters. Biotin-containing fragments were isolated using streptavidin beads before PCR
156 enrichment of each library. The library was sequenced on an Illumina HiSeqX platform to
157 produce approximately 30x sequence coverage.

158

159 The input *de novo* assembly was the *Z. indianus* “RCR04” PacBio assembly (assembly
160 # ASM1890459v1) from Kim et al. (2021). This assembly and Dovetail OmniC library reads
161 were used as input data for HiRise, a software pipeline designed specifically for using
162 proximity ligation data to scaffold genome assemblies (Putnam et al. 2016). Dovetail OmniC
163 library sequences were aligned to the draft input assembly using *bwa* (Li and Durbin 2009).
164 The separations of Dovetail OmniC read pairs mapped within draft scaffolds were analyzed by
165 HiRise to produce a likelihood model for genomic distance between read pairs, and the model
166 was used to identify and break putative misjoins, to score prospective joins, and make joins
167 above a threshold. See Figure S1 for link density histogram of scaffolding data.

168

169 *Annotation*

170

171 Repeat families found in the genome assemblies of *Z. indianus* were identified *de novo* and
172 classified using the software package *RepeatModeler* v. 2.0.1 (Flynn et al. 2020).

173 *RepeatModeler* depends on the programs *RECON* v. 1.08 (Bao and Eddy 2002) and
174 *RepeatScout* v. 1.0.6 (Price et al. 2005) for the de novo identification of repeats within the
175 genome. The custom repeat library obtained from *RepeatModeler* was used to discover,
176 identify and mask the repeats in the assembly file using *RepeatMasker* v. 4.1.0 (Smit et al.
177 2015).

178
179 RNA sequencing was conducted on 3 replicates of 3rd instar larva and 3 replicates of
180 mixed stage pupa that were snap frozen in liquid nitrogen. RNA extraction and sequencing
181 was performed by GeneWiz (South Plainfield, NJ). New larval and pupal RNAseq reads were
182 combined with adult RNA sequencing from Comeault et al. (2020) for annotation. Coding
183 sequences from *D. grimshawi*, *D. melanogaster*, *D. pseudoobscura*, *D. virilis*, *Z. africanus*, *Z.*
184 *indianus*, *Z. tsacasi* and *Z. tuberculatus* (Kim et al. 2021) were used to train the initial *ab initio*
185 model for *Z. indianus* using the *AUGUSTUS* software v. 2.5.5 (Keller et al. 2011). Six rounds of
186 prediction optimization were done with the software package provided by *AUGUSTUS*. The
187 same coding sequences were also used to train a separate *ab initio* model for *Z. indianus*
188 using *SNAP* (version 2006-07-28) (Korf 2004). RNAseq reads were mapped onto the genome
189 using the *STAR* aligner software (version 2.7) (Dobin et al. 2013) and intron hints generated
190 with the *bam2hints* tools within *AUGUSTUS*. *MAKER* v. 3.01.03 (Cantarel et al. 2008), *SNAP*
191 and *AUGUSTUS* (with intron-exon boundary hints provided from RNAseq) were then used to
192 predict for genes in the repeat-masked reference genome. To help guide the prediction
193 process, Swiss-Prot peptide sequences from the UniProt database were downloaded and used
194 in conjunction with the protein sequences from *D. grimshawi*, *D. melanogaster*, *D.*
195 *pseudoobscura*, *D. virilis*, *Z. africanus*, *Z. indianus*, *Z. tsacasi* and *Z. tuberculatus* to generate
196 peptide evidence in the *MAKER* pipeline. Only genes that were predicted by both *SNAP* and
197 *AUGUSTUS* were retained in the final gene sets. To help assess the quality of the gene
198 prediction, AED scores were generated for each of the predicted genes as part of the *MAKER*
199 pipeline. Genes were further characterized for their putative function by performing a BLAST
200 search of the peptide sequences against the UniProt database. tRNA were predicted using the
201 software *tRNAscan-SE* v. 2.05 (Chan and Lowe 2019). Transcriptome completeness was
202 assessed with *BUSCO* v. 4.0.5 (Manni et al. 2021) using the eukaryota_odb10 list of 255
203 genes.

204 205 *Wild fly collections*

206
207 Flies were collected by aspiration and netting from Carter Mountain Orchard, VA (37.9913° N,
208 78.4721° W) in 2017-2020 and from Hanover Peach Orchard, VA (37.5694° N, 77.2660° W) in
209 2019-2020. Flies were sampled from Coral Gables, FL (25.7239° N, 80.2802° W) in June 2019
210 using traps baited with bananas, oranges, yeast, and red wine. Flies were frozen in 70%
211 ethanol at -20°C (2017-2018) or dry at -80 °C (2019-2020) prior to sequencing. Collections
212 performed in July and August were called “early season.” In 2019, the earliest collections were
213 not made until September (typically when *Z. indianus* abundance peaks, Rakes *et al.* 2023),
214 and were assigned “mid-season.” Collections from October and November were called “late
215 season.” For some analyses, the mid-season collection and early collections were combined,

216 as they were the first collections available each year. See Table S1 for the number of
217 individual flies sequenced from each location and timepoint.

218

219 *Individual whole genome sequencing*

220

221 The sex of each wild-caught fly was recorded, then DNA was extracted from individual flies
222 using the DNAdvance kit (Beckman Coulter, Indianapolis, IN) in 96 well plates, including an
223 additional RNase treatment step. DNA concentration was measuring using the QuantIT kit
224 (Invitrogen, Waltham, MA) and purified DNA was diluted to 1 ng/μL. Libraries were prepared
225 from 1 ng of genomic DNA using a reduced-volume dual-barcoding Nextera (Illumina, San
226 Diego, CA) protocol as previously described (Erickson et al. 2020). The libraries were
227 quantified using the QuantIT kit and equimolar ratios of each individual DNA were combined
228 for sequencing. The pooled library was size-selected for 500 bp fragments using a BluePippin
229 gel cassette (Sage Sciences, Beverly, MA). The pooled libraries were sequenced in one
230 Illumina NovaSeq 6000 lane using paired-end, 150 bp reads by Novogene (Sacramento, CA).

231

232 Existing raw reads from *Z. indianus* collections from North America, South America, and
233 Africa (Comeault et al. 2020; Comeault et al. 2021) were downloaded from the SRA from
234 BioProject number PRJNA604690. These samples were combined with the new sequence
235 data and processed together with the same mapping and SNP-calling pipeline. Overlapping
236 paired-end reads were merged with *BBMerge* v. 38.92 (Bushnell et al. 2017). Reads were
237 mapped to the genome assembly described above using *bwa mem* v. 0.7.17 (Li and Durbin
238 2009). Bam files for merged and unmerged reads were combined, sorted and de-duplicated
239 with *Picard* v. 2.26.2 (<https://github.com/broadinstitute/picard>).

240

241 We next used *Haplotype Caller* from *GATK* v. 4.2.0.0 (McKenna et al. 2010) to generate
242 a gVCF for each individual. We built a GenomicsDBI database for each scaffold, then used this
243 database to genotype each gVCF. We used *GATK*'s hard filtering options to filter the raw
244 SNPs based on previously published parameters (`--filter-expression "QD < 2.0 || FS > 60.0 ||`
245 `SOR > 3.0 || MQ < 40.0 || MQRankSum < -12.5 || ReadPosRankSum < -8.0"`) (Comeault et al.
246 2020). We then removed SNPs within 20 bp of an indel from the output and removed all SNPs
247 in regions identified by *RepeatMasker*. We analyzed several measures of individual and SNP
248 quality using *VCFTools* v. 0.1.17 (Danecek et al. 2011). We removed 16 individuals with mean
249 coverage < 7X or over 10% missing genotypes. Next, we filtered SNPs with mean depths <10
250 or > 50 across all samples. We removed individual genotypes supported by 6 or fewer reads or
251 with more than 100 reads to produce a final VCF with 5,185,389 SNPs and 2,099,147 non-
252 singleton SNPs. See Table S1 for the final number of individuals included in the analysis from
253 each population. See Figure S2 for the average SNP depth per sampling time and location.

254

255 *Sex chromosome and Muller element identification*

256

257 *samtools* v. 1.12 (Li et al. 2009) was used to measure coverage and depth of mapped reads
258 from individual sequencing. This analysis revealed that the five main scaffolds (all over 25 Mb

259 in length) had a mean depth of ~16X coverage in both males and females in our dataset,
260 except for scaffold 3, which had ~16X coverage in females but ~8X coverage in males,
261 suggesting it is the X chromosome (Figure S3). Some of the previously sequenced samples
262 had no sex recorded, so we used the ratio of X chromosome reads (scaffold 3) to autosome
263 (scaffolds 1, 2, 4 and 5) reads to assign sexes to those individuals. Individuals with a ratio
264 greater than 0.8 were assigned female, and ratios less than 0.8 were assigned male (Figure
265 S4). For two known-sex individuals, the sex recorded prior to sequencing did not match the
266 sex based on coverage; for those two samples we used the coverage-based sex assignment
267 for analyses. We used D-GENIES (Cabanettes and Klopp 2018) to create dot-plots comparing
268 the *Z. indianus* and *D. melanogaster* genome (BDGP6.46, downloaded from ensemble.org) to
269 confirm the sex chromosome identification and assign Muller elements to *Z. indianus*
270 autosomes (Figure S5, Table S2). Five additional scaffolds had lengths over 1 Mb. Scaffold 8
271 is the dot chromosome (Muller element F) based on sequence comparison to *D. melanogaster*
272 (Figure S5) and had similar coverage to the autosomes (Figure S3). Scaffolds 6,7,9, and 10
273 had reduced coverage (Figure S3) and contain mostly repetitive elements. Downstream SNP
274 calling and population genetic analysis included the five large scaffolds (named chromosomes
275 1-5) and excluded all smaller scaffolds.

276

277 *Related individuals*

278

279 Preliminary exploration of population genetic data indicated that some individual samples may
280 be close relatives. For downstream analyses, we used the `-king-cutoff 0.0625` argument in
281 *Plink* v. 2.0 (Chang et al. 2015) to generate a list of unrelated individuals. This filtering
282 removed 21 individuals from the dataset. To quantify relatedness between all individuals, we
283 used the function `snpGdsibdKING` in *SNPRelate* v. 1.38.0 (Zheng et al. 2012) to determine the
284 kinship coefficients and probability of zero identity by descent for pairs of individuals using
285 autosomal SNPs. We used thresholds established in Thornton *et al.* (2012) to classify
286 relatedness between individuals.

287

288 *Population structure and F_{ST}*

289

290 We conducted principal components analysis using the R package *SNPRelate* v. 1.38.0
291 (Zheng et al. 2012) in R v. 4.1.1 (R Core Team) using a vcf that excluded singleton SNPs. We
292 LD pruned SNPs with a minor allele frequency of at least 0.05 using *SNPgdsLDpruning* with an
293 LD threshold of 0.2 and then calculated principal components with *snpGdsPCA* using all four
294 autosomes. For subsequent analyses, we repeated the LD pruning within subsets of the data
295 (North America only, or Carter Mountain, VA only). We also calculated principal components
296 using individual chromosomes; for the X chromosome, only females were used in the analysis.
297 We used t-tests and one-way ANOVAs followed by Tukey post-hoc tests to compare PC
298 values between sampling locations and time points.

299

300 We used *Plink* v. 1.9 (Purcell et al. 2007; Chang et al. 2015) to LD prune VCF files with
301 parameters (`--indep-pairwise 1000 50 0.2`) and used *ADMIXTURE* v. 1.3.0 (Alexander and

302 Lange 2011) to evaluate population structure for each chromosome separately. For the X
303 chromosome, only females were used. We tested up to $k=10$ genetic clusters and used cross-
304 validation analysis to choose the optimal k for each chromosome separately.

305

306 We calculated F_{ST} between Florida samples and early season Virginia samples using
307 the *snpGDSFST* function in *SNPRelate* for all SNPs with a minor allele frequency > 0.01 . For
308 the X chromosome, only females were used in F_{ST} calculations to ensure diploid genotypes.
309 We used the same function to calculate genome-wide, pairwise F_{ST} between all Virginia
310 collections using autosomal SNPs.

311

312 *Testing for structural variants*

313

314 We used *smoove* v. 0.2.6 (Pedersen et al. 2020) to identify and genotype insertions, deletions,
315 and rearrangements in the paired-end sequencing data from all individuals as described in the
316 documentation. We also used linkage disequilibrium (LD) of randomly sampled SNPs from
317 each chromosome to visually inspect for linkage due to potential inversions. We generated a
318 list of SNPs segregating in each focal population with no missing genotypes and randomly
319 sampled 4,000 SNPs from each chromosome. We used the *snpGDSLDMat* function in
320 *SNPRelate* to calculate LD between all pairs of SNPs. LD heatmaps were created with the
321 *ggLD* package (<https://github.com/mmkim1210/ggLD>).

322

323 *Estimation of historic population sizes*

324

325 We used *smc++* v. 1.15.4 (Terhorst et al. 2017) to estimate historic population sizes for several
326 subpopulations of individuals using autosomal genotypes. We used individuals from each
327 African location and used the earliest sampling available for each year and Virginia orchard.
328 We used *vcf2smc* to prepare the input files for each autosome separately. We assigned each
329 individual as the “distinguished individual” and ran the analysis using all possible combinations
330 of distinguished individual as described in (Bemmels et al. 2021). We used 10-fold cross
331 validation to estimate final model parameters with the option (*-cv -folds 10*). We assumed a
332 generation time of 0.08 years (~12 generations per year) based on Nava *et al.* (2007), which
333 assumes year-round reproduction in tropical regions. We note that for Virginia populations
334 experiencing temperate conditions in recent years, 12 generations per year is likely an
335 overestimate due to the shortened breeding season.

336

337 *Selection scan*

338

339 We used *WhatsHap* v. 1.7 (Patterson et al. 2015) to perform read-based phasing of the full vcf
340 including singletons. To polarize the vcf for the genome wide selection scan relative to the
341 invasion, we reassigned the reference allele of the phased vcf as the allele that was most
342 common across all African individuals sequenced in previous studies. We calculated allele
343 frequencies using all African samples in *SNPRelate*, then used *vcf-info-annotator*
344 (<https://vatools.readthedocs.io/en/latest/index.html>) to assign the “ancestral” allele in the INFO

345 column. Lastly we used *bcftools* v. 1.13 (Danecek et al. 2021) to make simplified vcfs
346 containing only the GT and AA fields for each chromosome separately.

347

348 We used the R package *rehh* v. 3.2.2 (Gautier and Vitalis 2012) to conduct the selection
349 scan using integrated haplotype homozygosity score. We split samples into four possible
350 populations (Africa, Florida, all North America, Virginia only) and conducted the scans
351 separately for each population using phased, polarized vcfs for each individual chromosome.
352 We used the *haplo2hh*, *scan*, and *ihh2ihs* functions to implement the scan. For the X
353 chromosome, we only used a single haplotype for each male in the dataset to avoid double
354 counting haploid genotypes. Haplotypes under selection were visualized by plotting all SNPs
355 with IHS > 5. LD between candidate SNPs was calculated in *SNPRelate*.

356

357 *Genetic diversity statistics*

358

359 Because we obtained variable sequencing coverage within and across populations (Figure S2)
360 we used software designed for low coverage and missing data to analyze population genetic
361 statistics in genomic windows. We used *pixy* v. 1.2.5 (Korunes and Samuk 2021) to calculate
362 π , F_{ST} and D_{XY} in 5 kb windows. Samples were grouped by collection location and year or by
363 collection location for different analyses. We used *ANGSD* v. 0.941 (Korneliussen et al. 2014)
364 to calculate Tajima's D. We first calculated genotype likelihoods from the bam files using
365 arguments *-doSaf* and *-GL*. We then calculated Tajima's D and theta using the folded site
366 frequency spectrum across 5 kb windows with 5 kb steps as described in *ANGSD*
367 documentation.

368

369 *Data management and plotting*

370

371 We used the R packages *foreach* (Microsoft and Weston 2017) and *data.table* (Dowle and
372 Srinivasan 2019) for data management and manipulation and used *ggplot2* (Wickham 2016)
373 for all plotting. The *ggpubfigs* (Steenwyk and Rokas 2021) and *viridis* (Garnier 2018) packages
374 were used for color palettes.

375

376 **Results and Discussion**

377

378 *Genome assembly and annotation*

379

380 High quality genome assemblies and annotations are a critical component of tracking and
381 controlling invasive species and understanding the potential evolution of invasive species in
382 invaded ranges (Matheson and McGaughan 2022). We conducted Hi-C based scaffolding of a
383 previously sequenced *Z. indianus* genome (Kim et al. 2021) to achieve a chromosome-level
384 assembly. There were 1,014 scaffolds with an N50 of 26.6 Mb, an improvement from an N50
385 of 4.1-6.8 Mb in previous assemblies (Kim et al. 2021). The five main chromosomes (Figure
386 S1, named in order of size from largest to smallest) varied in length from 25.7 to 32.3 Mb (total
387 length of five main scaffolds = 146,062,119 bp), in agreement with *Z. indianus* karyotyping

388 (Gupta and Kumar 1987; Campos et al. 2007). Chromosome 3 was identified as the sex
389 chromosome using sequencing coverage of known-sex individuals (Figure S3, S4) and
390 sequence comparison dot-plots (Figure S5). See Table S2 for assignment of *Z. indianus*
391 chromosomes to Muller elements based on alignment to the *D. melanogaster* genome.

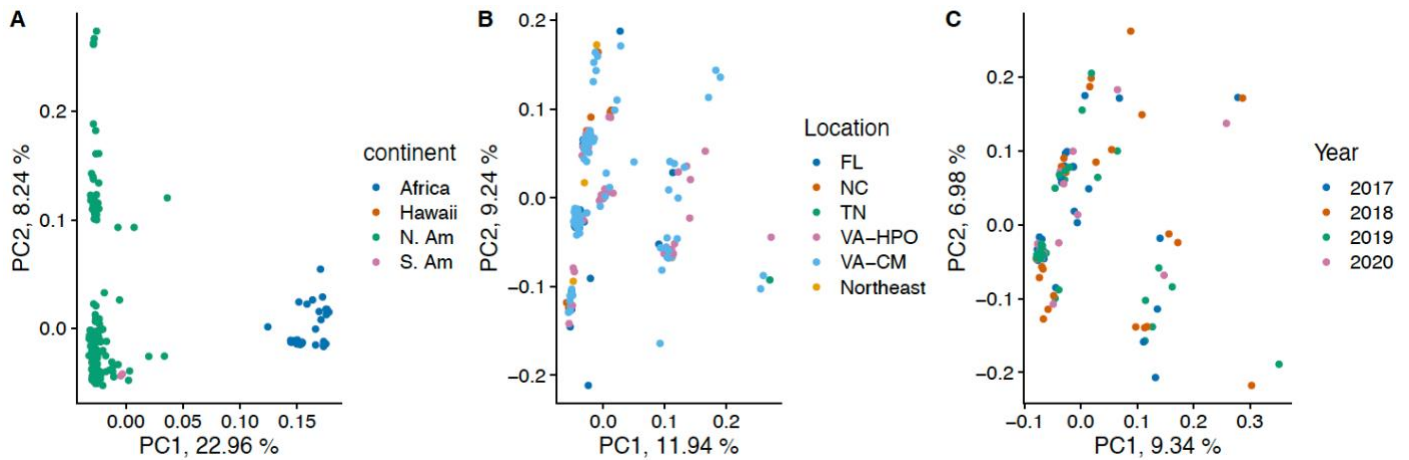
392
393 The annotation using RNAseq from larvae, pupae, and adults predicted 13,162
394 transcripts and 13,075 proteins, with 93% of 255 benchmarking universal single copy orthologs
395 (BUSCO) genes (Simão et al. 2015) identified as complete and an additional 1.2% of BUSCO
396 genes identified as fragmented. This transcriptome-based completeness estimate is lower than
397 the genome-based estimate of 99% complete (Kim et al. 2021) but is in line with other
398 arthropod genomes (Feron and Waterhouse 2022). Within the 5 main scaffolds, 24.6% of
399 sequences were repetitive; within the entire assembly including all smaller scaffolds, 41% were
400 repetitive. The five main chromosomes contain 11,327 predicted mRNAs (87% of all
401 predicted), including 99.5% of all complete BUSCO genes. This improved genome resource
402 will be valuable for future evolutionary studies of *Z. indianus*, which is becoming an
403 increasingly problematic pest in some regions of the world (Allori Stazonelli et al. 2023).

404
405 *Limited spatial or temporal population structure in North American Z. indianus*

406
407 To study spatial and temporal patterns of genetic variation in the seasonally repeated invasion
408 of *Z. indianus*, we resequenced ~220 individuals collected from two orchards in Virginia
409 (Charlottesville and Richmond) from 2017-2020, as well as one population collected from
410 Miami, Florida in 2019. Because temperate locations such as Virginia are thought to be
411 recolonized by *Z. indianus* each year (Pfeiffer et al. 2019; Rakes et al. 2023), we sampled both
412 early in the season (~July-August) and late in the season (~October-November) in each year
413 to capture the founding event, population expansion, and potential adaptation to the temperate
414 environment.

415
416 We were first interested in studying geographic and temporal variation in population
417 structure in North American populations of *Z. indianus*. For this analysis, we incorporated
418 previous sequencing data from the Western Hemisphere and Africa (Comeault et al. 2020).
419 While previous studies have shown limited structure within North America (Comeault et al.
420 2020; Comeault et al. 2021), we wanted to test for structure using deeper sampling within
421 introduced locations and with greater temporal resolution across the *Z. indianus* growing
422 season (Rakes et al. 2023). As shown previously, in an autosome-wide principal component
423 analysis, PC1 separated Western Hemisphere and African samples (Figure 1A; t-test: $t =$
424 78.92 , $df = 36$, $p < 2 \times 10^{-16}$). However, with the increased sample size of North American flies
425 relative to previous studies, PC2 separated North American samples into two clusters,
426 explaining 8% of total variation. To focus on potential structure within invasive North American
427 samples, we excluded the African samples and recalculated principal components. This
428 analysis revealed little genome-wide differentiation of North American populations collected
429 from different locations (Figure 1B; ANOVA $P > 0.05$ for PC1 and PC2), though the samples

430 did fall into three large groups based on PC1, which may be indicative of structural variation (Li
431 and Ralph 2019); see below.
432



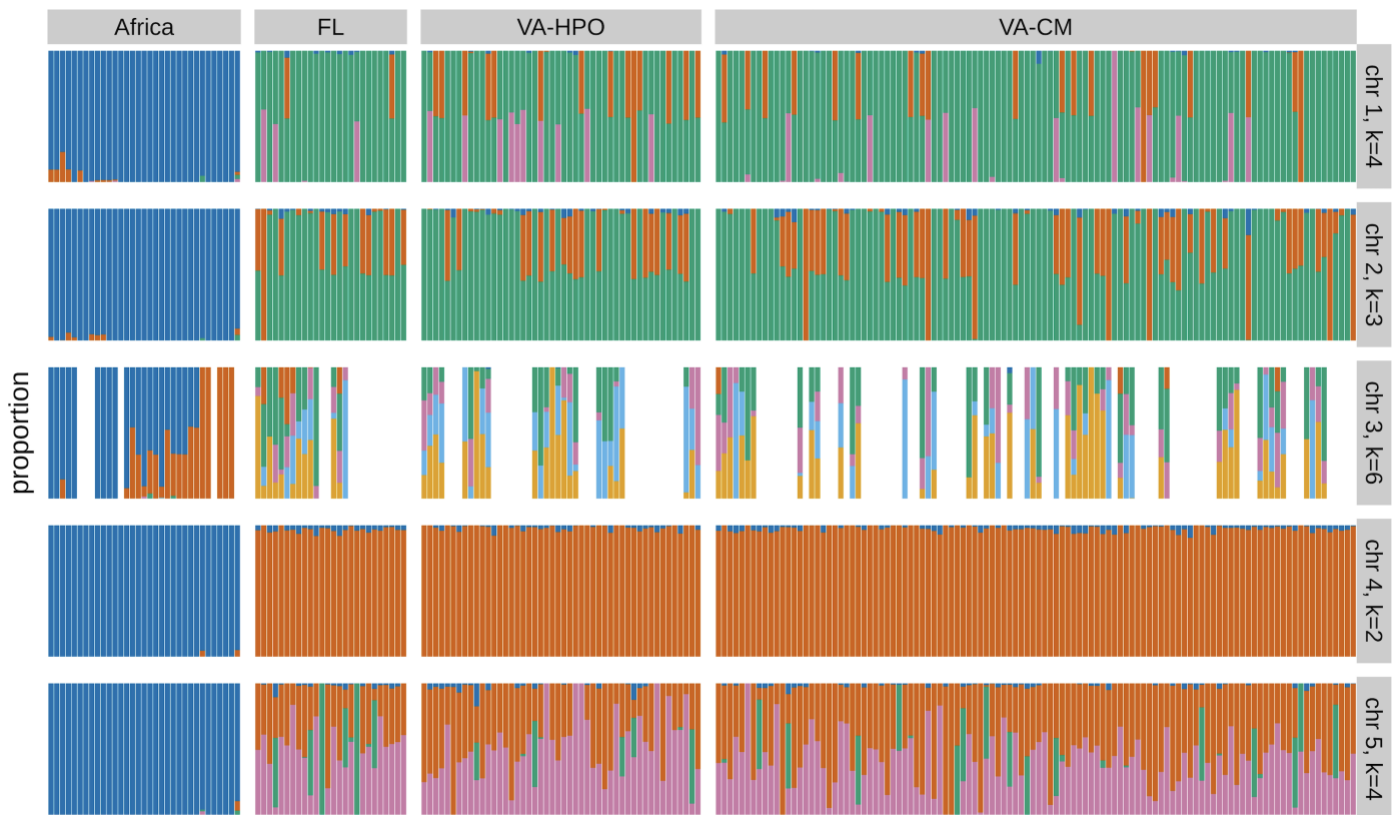
433
434 **Figure 1: Principal component analysis of individual *Z. indianus* from this**
435 **study and previous studies using autosomal SNPs.** (A) All unrelated
436 individuals ($n=247$), color coded by continent/locale of collection. (B). All
437 unrelated North American individuals ($n=190$), color coded by collection site;
438 HPO and CM are two orchards in Virginia; Northeast refers to samples from NY,
439 NJ, and PA. (C) All unrelated individuals from Carter Mountain, Virginia ($n=110$),
440 color coded by year of collection. For each analysis, only the individuals shown in
441 the plot were included in the PC calculation.
442

443 North American samples clustered in single-chromosome PCA for chromosomes 1, 2
444 and 5, but these clusters generally did not correspond to sampling locations (Figure S6; PC2
445 separated the two Virginia orchards for chromosome 5; Tukey $P = 0.01$). Interestingly, PC1
446 separated Florida from both Virginia orchards for the X chromosome (Tukey $P < 0.01$ for each
447 comparison), suggesting some degree of genetic differentiation on the X. Visual inspection of
448 plots of PC3 and PC4 did not indicate additional geographic population structure (results not
449 shown). The overall lack of genome- or chromosome-wide geographic population structure
450 suggests that there is not a high degree of genetic differentiation between eastern North
451 American populations spread over a latitudinal transect (~1600 km) encompassing distinct
452 climates, but some localized patterns of population structure may exist on the X chromosome.
453 Many invasive species evolve complex population structures in the invaded range due to a
454 combination of bottlenecks, founder effects and rapid local adaptation (Koch et al. 2020;
455 Atsawawaranunt et al. 2023; García-Escudero et al. 2023). On the other hand, some invasive
456 species have more homogenous populations across widespread invaded ranges in eastern
457 North America (Friedline et al. 2019; Barrett et al. 2023). A high rate of migration between
458 orchards (occurring naturally or due to human-mediated transport) or large founding population
459 sizes could result in a lack of geographic differentiation between populations.
460

461 We next hypothesized that founder effects during each recolonization event might lead
462 to unique genetic compositions of temperate populations sampled in different years (Uller and

463 Leimu 2011). We calculated principal components using only samples collected from Carter
464 Mountain, VA in 2017-2020. Surprisingly, in these samples, we saw no evidence of population
465 structure between years across the genome (Figure 1C; ANOVA $P > 0.05$ for PC1 and PC2) or
466 on individual chromosomes, except for chromosome 4, which showed subtle separation of
467 some years (Figure S6; Tukey $P < 0.05$ for PC1: 2018 vs. 2019 and PC2: 2017 vs. 2019).
468 These data suggest that the founding fly populations in Virginia are relatively homogeneous
469 each year at a genome-wide scale. This result is consistent with the lack of spatial population
470 structure and likewise could indicate large founding populations or ongoing migration.
471 Alternatively, the Virginia population could be permanently established with little genetic
472 differentiation year-to-year, though this possibility is not supported by field data (Rakes et al.,
473 2023).

474
475 We used ADMIXTURE (Alexander and Lange 2011) to test for population structure
476 using individuals from Africa, Florida, and the two focal Virginia orchards, calculating the most
477 likely number of genetic clusters for each chromosome separately. Consistent with the PCA,
478 the four autosomes each produced between two to four genetic groups, but there was no
479 apparent geographic population structure, aside from African samples mostly belonging to
480 different clusters from all North American samples for each chromosome (Figure 2). Notably,
481 for chromosomes 1 and 2, many individuals showed ~50% ancestry assignment to different
482 clusters, which could reflect genotypes for large structural rearrangements (see below). For the
483 X chromosome, using females only, we identified structure within African samples as
484 previously described (Comeault et al. 2020; Comeault et al. 2021) and a total of five genetic
485 clusters within North American populations, including one of the African genetic groups which
486 was found in Florida (Figure 2 third row; see orange grouping). X chromosomes have smaller
487 effective population sizes in species with XY sex determination systems and often experience
488 more extreme loss of genetic diversity upon population contraction (Ellegren 2009). The
489 complex population structure seen on the X chromosome may be the result of this small
490 population size or caused by selection on X-linked variants in different environments.
491



492

493

494

495

496

497

498

499

500

501

502

503

504

505

506

507

508

509

510

511

512

513

514

Figure 2: Admixture analysis of individual *Z. indianus* chromosomes from different locations. Each column is an individual, and colors represent assignment to distinct genetic clusters. The most likely number of genetic clusters for each chromosome (k) was obtained with cross-validation analysis and is shown at right. For chromosome 3, the X chromosome, only female flies were used for admixture analysis, resulting in reduced sample size. FL=Miami, Florida, VA-HPO = Richmond, VA, VA-CM = Charlottesville, VA. African sequences represent five geographic locations and are taken from Comeault et al. (2020 & 2021).

Structural polymorphism

The clustering of samples in the single-chromosome PCA (Figure S6), combined with many individuals showing ~50% assignment to genetic clusters (Figure 2), suggested that large structural variants may be segregating in *Z. indianus* (Li and Ralph 2019; Nowling et al. 2020). Analysis of paired-end sequencing data with *smoove* provided evidence of two large rearrangements on chromosome 1 located at 7.1 and 9.1 Mb; the genotypic combinations for these variants largely correlate with the clustering of samples in the PCA (Figure S7; PC1 correlation with variant at 7.1Mb: $P = 2 \times 10^{-9}$; PC1 correlation with variant at 9.1Mb: $P = 3 \times 10^{-5}$; PC2 correlation with variant at 9.1Mb: $P = 0.001$). Since chromosome 1 is the longest chromosome in our assembly, these rearrangements likely correspond to the complex *In(IV)EF* polymorphism, made up of two overlapping inversions (Ananina et al. 2007). *smoove* did not

515 identify large structural variants on chromosomes 2 or 5 whose genotypes correlated to the
516 PCA clusters.

517

518 To look for evidence of structural variants via depressed recombination rates, we
519 examined linkage disequilibrium (LD) from 4,000 randomly sampled SNPs on each
520 chromosome. In North American samples, we discovered large blocks of LD spanning
521 substantial portions of chromosomes 1, 2, 3, and 5 (Figure S8), potentially indicative of
522 inversions (Fang et al. 2012; da Silva et al. 2019). However, there was no evidence of long-
523 distance LD in these regions in the African samples (Figure S8). *smoove* did not identify
524 inversions that corresponded to the sizes and locations of these linkage blocks. These results
525 support the read-based evidence of a complex rearrangement on chromosome 1 (Figure S7)
526 and suggest inversions on chromosomes 1, 2, 3, and 5 are segregating in North America but
527 are relatively rare in Africa. Given the relative chromosome sizes in the genome assembly, the
528 linkage blocks on chromosome 2 and 5 likely correspond to *In(V)B* and *In(II)A*, respectively
529 (Ananina et al. 2007). The X chromosome has three described inversions in *Z. indianus*
530 (Ananina et al. 2007), which may explain to the complex pattern of linkage observed in North
531 American samples and the population structure observed for the X chromosome within North
532 America (Figure 2). Major chromosomal polymorphisms are known to be important for local
533 adaptation and phenotypic divergence in a wide variety of species (Joron et al. 2011; Küpper
534 et al. 2016; Lee et al. 2016; Huang et al. 2020; Nunez et al. 2024), including inversions that
535 facilitate invasive phenotypes (Galludo et al. 2018; Tepolt and Palumbi 2020; Tepolt et al.
536 2022; Ma et al. 2024). These inversions may have been present at low frequency in the
537 bottlenecked population that founded *Z. indianus* populations in the Western Hemisphere, but
538 then experienced subsequent selection in the invaded range. Alternatively, these
539 polymorphisms may have arisen in a currently undescribed population and then been
540 introduced to the Western Hemisphere.

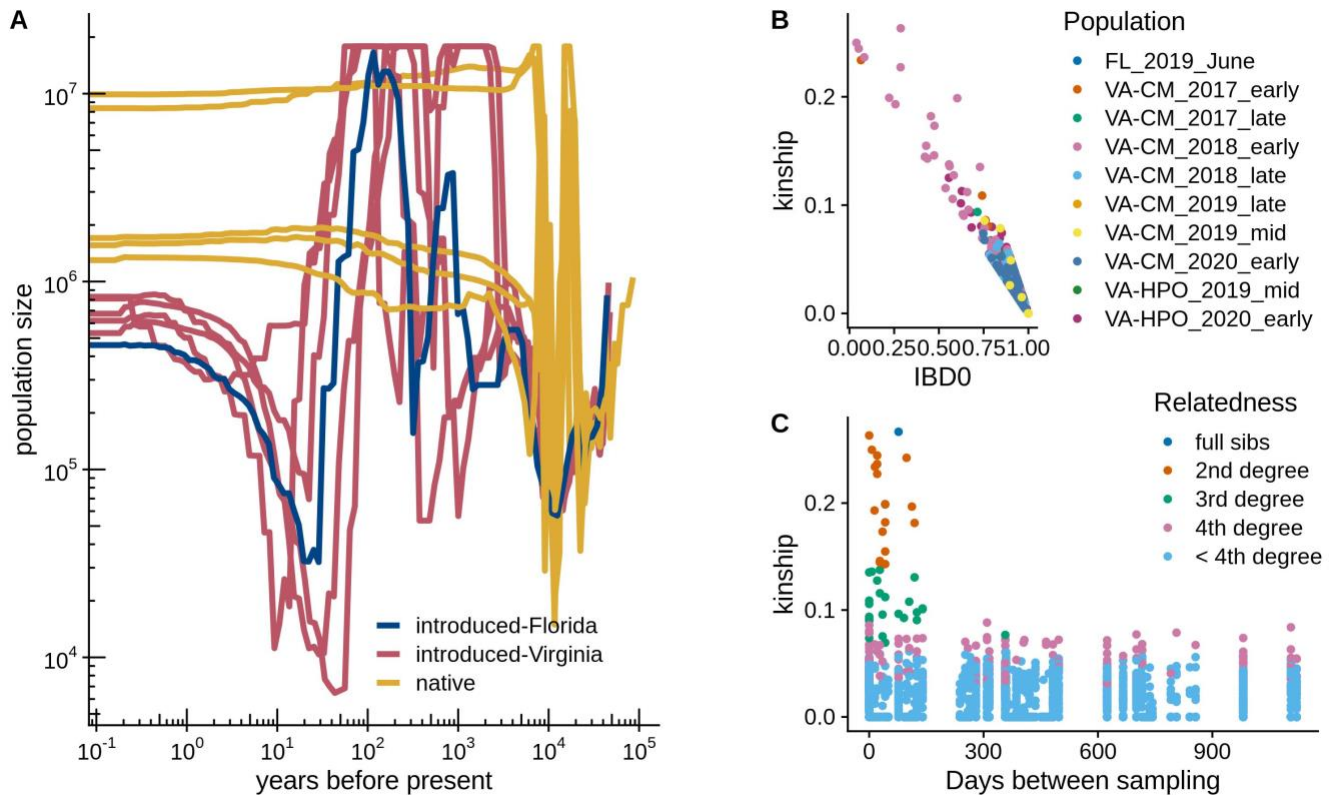
541

542 *Recolonization, bottlenecks and seasonal dynamics in Z. indianus*

543

544 Invasive species typically experience a genetic bottleneck due to small founding population
545 sizes (Barrett 2015; Estoup et al. 2016). We hypothesized that North American populations
546 would show reduced effective population size (N_e) relative to African populations, and that
547 Virginia populations would show a further, more recent reduction in N_e relative to Florida
548 populations as the result of a secondary population bottleneck upon temperate recolonization.
549 Our prediction was correct with respect to Africa vs North America: African populations show
550 historical fluctuations but population sizes typically in the range of $\sim 10^5$ - 10^7 individuals.
551 Interestingly, introduced populations in North America demonstrate population sizes that
552 increased, decreased, then increased again in the past ~ 500 years. Comeault et al. (2021)
553 suggested that introduced populations in the Americas are derived from a historically admixed
554 population composed of both East African and West African flies, and the historic expansion of
555 introduced populations might correspond to this admixture event. The subsequent drop in
556 population size to 10^4 - 10^5 may then reflect a bottleneck following colonization of Brazil in the
557 late 1990s (Yassin et al. 2008), followed by a rebound as introduced populations expanded.

558



559

560

561

562

563

564

565

566

567

568

569

570

571

572

573

574

575

576

577

578

579

580

581

582

Figure 3: Demographic effects of bottlenecks in *Z. indianus* populations A)

Population history reconstruction with smc++ using autosomal genotypes. Introduced-Florida flies were collected in Miami in 2019. Introduced-Virginia flies were collected in the early-mid season (June-September) from two Virginia orchards in 2017-2020 ($n=5$ populations grouped by orchard and year). Native populations are distinct African populations (Kenya, Zambia, Senegal-Forest, Senegal-Desert, and Sao Tome [Comeault et al 2020]). B) Kinship and probability of zero identity by descent for pairs of individual flies from the same collection location and season within North America calculated with autosomal SNPs. C) Kinship coefficients for pairs of individual flies collected at Carter Mountain Orchard, Virginia, as a function of the number of days between sampling. Relatedness was assigned according to thresholds from (Thornton et al. 2012).

Overall, the ancestral population sizes for Virginia and Florida were quite similar, and our prediction of reduced recent population sizes in Virginia relative to Florida was not well-supported. The minimum population sizes for Florida and Virginia (10^4 - 10^5) are larger than expected for a single small colonization event. Field data suggest founding populations in orchards are small and then rapidly expand (Rakes et al. 2023), suggesting that these large population sizes could be caused by ongoing gene flow from the source population after colonization, which is consistent with the lack of temporal population structure. Given our limited sample sizes and potential differences in the number of generations per year in

583 temperate and subtropical environments, detecting fine-scale differences in very recent
584 population fluctuations may be beyond the detection ability of the software; *smc++* becomes
585 less accurate at timescales less than ~133 generations (Patton et al. 2019). Alternatively, the
586 Virginia populations may be admixed populations reflecting individuals from multiple sources,
587 producing larger effective population sizes than would otherwise be expected if recolonization
588 occurs from a single source population undergoing a bottleneck. Admixture and gene flow are
589 important factors fueling genetic diversity and invasiveness in introduced species
590 (McGaughan et al. 2024) and could potentially contribute to *Z. indianus*' local success
591 following each recolonization event.

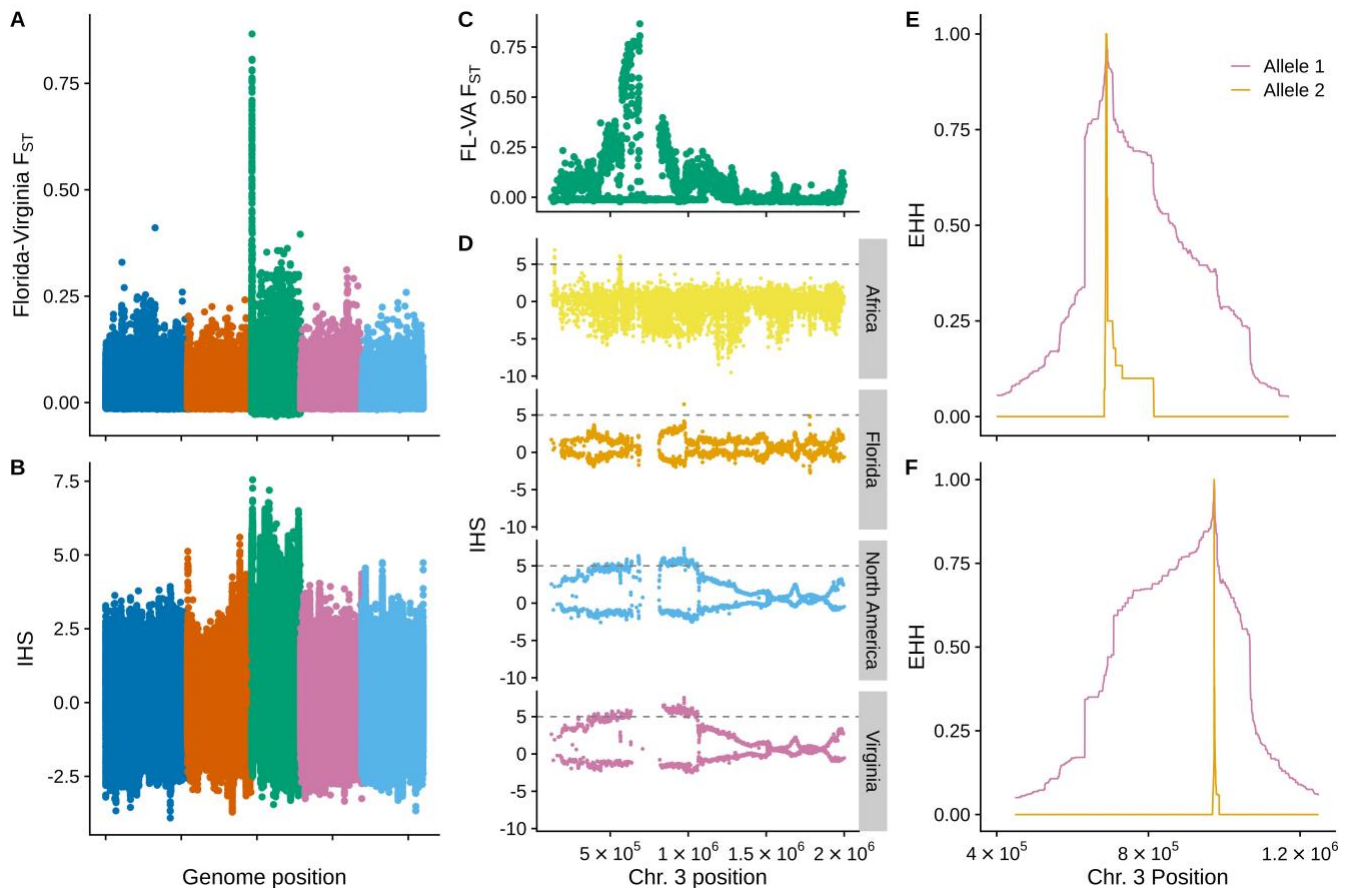
592
593 We additionally tested for bottlenecks by looking for inbreeding, which might be a
594 product of small founding populations. Using two measures of genetic similarity, we discovered
595 many pairs of related flies in our dataset (Figure 3B). Most dramatically, many flies collected in
596 2018 appeared to be close relatives (Figure S9). In collections from late July and early August
597 2018, 26 pairs of close relatives involving 13 individual flies were collected. Of those, 21 pairs
598 of relatives were collected on different days, suggesting the relatedness was not solely a
599 sampling artifact due to collecting closely related flies in the same microhabitat of the orchard.
600 The effect of this apparent bottleneck was sometimes retained throughout the growing season,
601 as a pair of full sibs was sampled 77 days apart in 2018, two pairs of second-degree relatives
602 were sampled over 110 days apart in 2018, and two pairs of third-degree relatives were
603 sampled 140 days apart in 2017 (Figure 3C). Given that *Z. indianus* are collected in small
604 numbers early in the season (Rakes et al. 2023) and 2017 and 2018 had particularly early
605 captures (Table S1), we suggest small founding population size followed by inbreeding could
606 produce individuals sampled distantly in time that still show close genetic similarity.
607 Alternatively, flies may live for a relatively long time or have slower generations in the wild,
608 allowing us to capture close relatives separated by longer time periods. However, we note that
609 the same pattern was not seen in every year of our collections, suggesting that colonization
610 dynamics might differ dramatically from year to year, which is expected if recolonization occurs
611 due to chance events each year.

612
613 The founder effect could generate temporal population structure by creating populations
614 that were more similar within a year than between years, creating a positive relationship
615 between F_{ST} and the elapsed time between collections (Bergland et al. 2014). We tested this
616 prediction with samples collected from Carter Mountain, Virginia over four years, and there
617 was no relationship between F_{ST} and the time between sampling (linear model, $df=17$, $P=0.9$,
618 Figure S10). This lack of temporal differentiation is consistent with the PCA and the relatively
619 large minimum population sizes previously described and could be produced by ongoing gene
620 flow that eliminates any signal of a founder effect and inbreeding. This finding is distinct from
621 trends observed in *D. melanogaster*, which experiences a strong overwintering bottleneck and
622 shows temporal patterns of differentiation (Bergland et al. 2014; Nunez et al. 2024).

623
624 *Repeated differentiation between Florida and Virginia populations*

625

626 Despite the lack of genome-wide differentiation between different North American locales, we
627 were interested in testing whether specific regions of the genome might differ between
628 populations given environmental differences: Virginia has a temperate, seasonal climate with a
629 relatively limited variety cultivated produce, and southern Florida is subtropical with an
630 abundance and diversity of fruits throughout the year. Other factors such as diseases,
631 insecticide use, and competing species may also differ widely between locales. In the absence
632 of genome-wide population structure, genomic regions differentiated between these locations
633 are candidates for local adaptation. We conducted a SNP-level F_{ST} analysis comparing all flies
634 collected in Florida to those collected in the early season in Virginia over four years. We
635 observed elevated F_{ST} throughout much of the X chromosome, with a pronounced peak at 690
636 kb (Figure 4A). This peak was observed when comparing the Florida collection to Virginia
637 collections from both Charlottesville and Richmond across all four years of Virginia sampling
638 both early and late in the season (Figure S11), suggesting that this differentiation is maintained
639 through recurrent rounds of recolonization, potentially via local adaptation. Alternatively, this
640 region could correspond to alleles that directly promote dispersion and/or invasion (Weinig et
641 al. 2007) and are found at higher frequency in invaded populations. One limitation of our
642 sampling strategy is that we have only a single year of sampling in Florida; additional data will
643 be needed to determine whether the genetic composition of this population (and differentiation
644 from Virginia) remains steady across multiple years. However, assuming that this result is not
645 an artifact related to the Florida sample, an alternative possible explanation for the repeated
646 differentiation seen between Florida and Virginia is that Virginia is recolonized by a source
647 population that is genetically distinct from the southern Florida population we sampled here.
648 Regardless, the finding implies localized genetic structure across a latitude gradient in North
649 American.
650
651



652
653 **Figure 4: Signals of selection in temperate *Z. indianus* populations.** A)
654 Genome-wide SNP-level F_{ST} comparing individual flies sampled in Florida (n=26)
655 to all flies sampled in the early season in Virginia (n=123), color-coded by
656 chromosome. Only females were used for the X chromosome (chromosome 3,
657 green). B) Integrated haplotype homozygosity score (IHS) using all flies collected
658 in Virginia. C) Zoomed in view of SNP-level F_{ST} between Florida and Virginia on
659 chr 3: 0-2Mb. D) IHS for the X chromosome (chromosome 3:0-2 Mb) calculated
660 separately for flies from Africa, Florida, all North America, and Virginia. Dashed
661 line indicates IHS = 5 to facilitate comparisons between populations. E-F)
662 Extended haplotype homozygosity for the two alleles of the SNP with highest F_{ST}
663 (E; chr 3: 689841) and highest IHS (F; chr 3: 973443), calculated using all
664 haplotypes from Virginia.

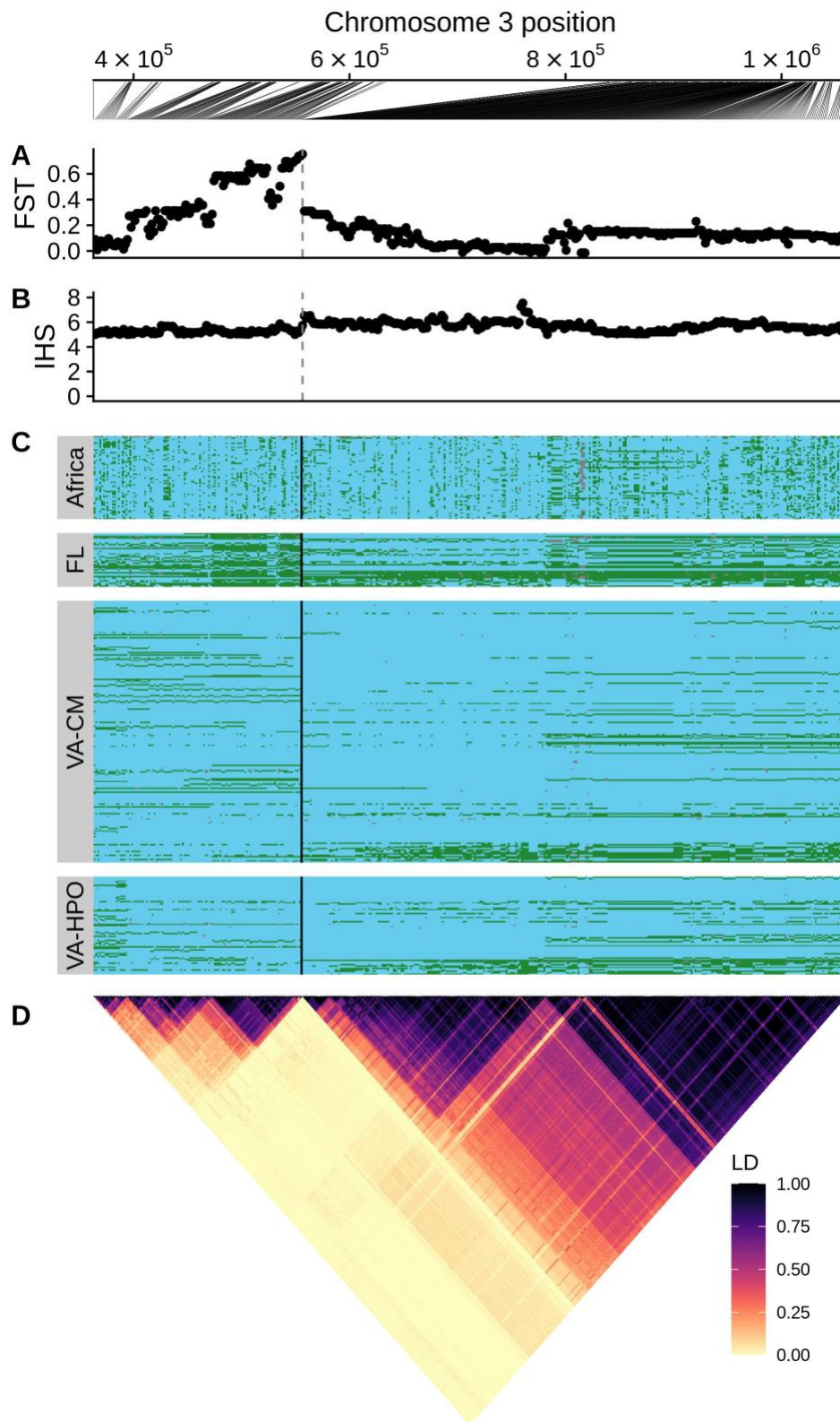
666 *Genomic signals of differentiation and selection*

667
668 The elevated F_{ST} seen on the X chromosome raised the intriguing possibility that some genetic
669 variation could potentially be under selection in temperate environments (Virginia) relative to
670 subtropical Florida. We phased the paired-end sequencing data and calculated extended
671 haplotype homozygosity (EHH) and IHS (integrated haplotype homozygosity score) using all
672 Virginia individuals to look for long, shared haplotypes that can be signatures of selective
673 sweeps (Sabeti et al. 2007). As in the F_{ST} analysis, we observed a region on chromosome 3

674 that stood out in this analysis with many SNPs with $IHS > 5$; this region overlapped with the
675 F_{ST} peak (Figure 4, B-D). The peak F_{ST} SNP was approximately 300 kb away from the peak
676 IHS SNP. We then repeated the IHS analysis using flies from Africa, Florida, and all North
677 America (Virginia + Florida + Comeault (2020) locations) to determine whether this signature
678 was unique to temperate populations. There was no signal of elevated IHS in African flies
679 (Figure 4D, 1st row), suggesting this selective signature is unique to invasive populations.
680 Further, this region showed a less substantial IHS peak when analyzing flies collected in
681 Florida (Figure 4D, 2nd row) but was prominent when examining Virginia flies or all North
682 American flies (Figure 4D, 3rd-4th rows), suggesting the signal of the selective sweep is
683 primarily driven by individuals collected in temperate environments. Both the peak IHS SNP
684 and the peak F_{ST} SNP showed evidence of long extended haplotypes characteristic of sweeps
685 (Figure 4E-F). These results further support the possibility that this locus is advantageous to
686 invasive potential or survival in temperate habitats.

687
688 We investigated this region of the genome by examining linkage disequilibrium (LD) and
689 haplotype structure of the 400 SNPs with a Virginia $IHS > 5$ (Figure 5A). We discovered this
690 region spanning ~700 kb has several large haplotype blocks in temperate North American
691 samples (Figure 5C-D) and in Florida (Figure S12B), but these same haplotypes are not found
692 in Africa (Figure 5C, Figure S12A), suggesting they are unique to introduced populations. In
693 invasive copepods, haplotypes under selection in the invasive range are ancestral
694 polymorphisms under balancing selection in the native range (Stern and Lee 2020). A similar
695 situation was found for a balanced inversion polymorphism that fuels invasion in invasive crabs
696 (Tepolt and Palumbi 2020; Tepolt et al. 2022). However, ancestral polymorphism selected in
697 the invaded range does not appear to be the case in *Z. indianus*, as the haplotypes from North
698 America were not found in any African flies. These novel haplotypes could be new mutations
699 or derived due to hybridization/introgression from another species or divergent population;
700 hybridization can be an important evolutionary force in invasive species (Ellstrand and
701 Schierenbeck 2000; Fournier and Aron 2021). The *Zaprionus* genus shows signals of historic
702 introgression, though *Z. indianus* was not directly implicated in a previous analysis (Suvorov et
703 al. 2022). Therefore, two major haplotypes not found in Africa contribute to the differentiation of
704 Florida and Virginia populations, though the source of these haplotypes remains to be
705 determined. Though we focus on one genomic region, we note that most of the X chromosome
706 shows elevated IHS scores (Figure 3B), and many SNPs on the X show $F_{ST} > 0.25$ between
707 Virginia and Florida (Figure 3A). This observation is in line with the findings of Comeault et al
708 2021, who showed that many X-linked scaffolds showed signs of selection in invasive
709 populations and is likely related to the presence of several inversions on this chromosome. We
710 also note that our approach would not detect sweeps involving multiple alleles from standing
711 variation (soft sweeps; (Messer and Petrov 2013; Garud et al. 2015)), which could be an
712 important potential component of *Z. indianus* evolution given the high levels of genetic diversity
713 found even in invasive populations (Avalos et al. 2017).

714



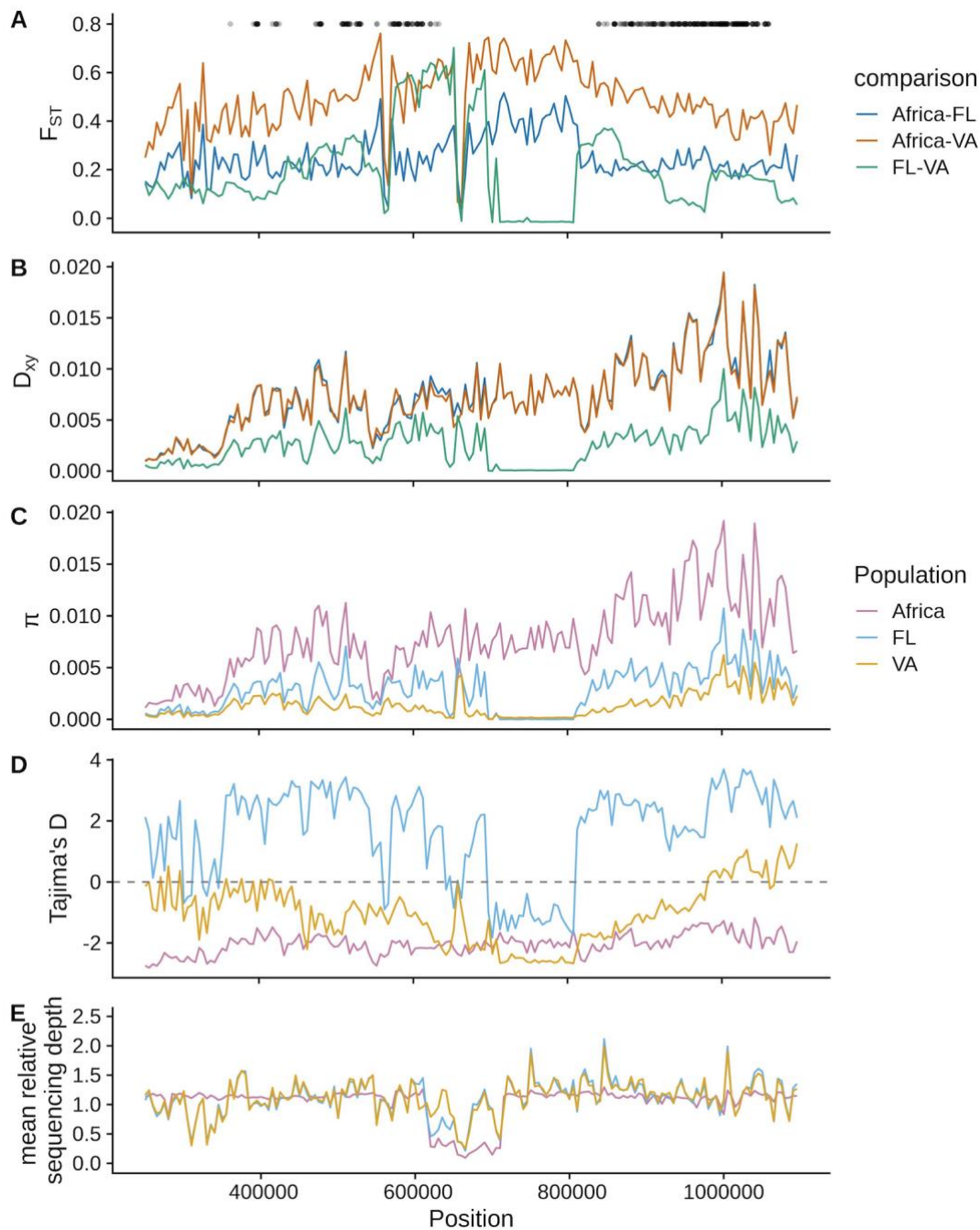
715
716
717
718
719
720

Figure 5: Major haplotypes on the X chromosome with signals of selection and differentiation. Only SNPs with IHS > 5 in Virginia (n=400) are shown in this figure for clarity; scale at top shows physical positions of SNPs, which are equally spaced in panels A-D. A) FST of individual SNPs comparing Florida and

721 *Virginia populations (see Figure 4). B) IHS for individual SNPs. C) Haplotypes:*
722 *each horizontal row shows genotypes for a single haploid chromosome phased*
723 *with read-backed phasing. Blue indicates the allele more common in African*
724 *populations and green is the other allele. Missing genotypes are shown in gray.*
725 *D) LD (R^2) for these SNPs in all North American flies, excluding Florida.*
726

727 To explore population genetic signals around this highly divergent region of the X
728 chromosome, we broadly grouped flies into three populations: Africa, Florida, and Virginia and
729 calculated population genetic statistics in 5 kb non-overlapping windows for all females. This
730 analysis confirmed two regions of relatively high F_{ST} between Florida and Virginia, though they
731 are separated by a region of nearly zero differentiation within North America, as measured by
732 F_{ST} , D_{xy} , and nucleotide diversity (Figure 6A-C, ~700-800kb). Virginia and Florida are both
733 highly differentiated from Africa in this region, and it has negative Tajima's D in both Florida
734 and Virginia (Figure 6D), potentially indicating recovery from a selective sweep in North
735 America. The region of no divergence may represent a selective sweep of a haplotype that
736 existed on two different genetic backgrounds that were subsequently favored in Florida and
737 Virginia, producing a high degree of genetic differentiation in the surrounding sequences. The
738 region with a potential sweep in North America contains ~6 genes, including the gene *yin/opt1*,
739 which is important for absorption of dietary peptides in *D. melanogaster* (Roman et al. 1998).
740 Allelic differences between African and invasive range flies in this gene could be involved in
741 adaptation to new diets in new environments.

742
743



744
745
746
747
748
749
750
751
752
753
754

Figure 6: Population genetic statistics for the region surrounding a selected haplotypes on chromosome 3 (250-1,100 kb). All statistics were calculated for 5 kb, non-overlapping windows. Black points at the top indicate the locations of the 400 SNPs shown in Figure 5. A) F_{ST} comparing combinations of flies from Africa, Virginia (both focal orchards combined) and Florida. B) Absolute nucleotide divergence (D_{xy}) for the same comparisons. C) Nucleotide diversity (π) for each population. D) Tajima's D for the three populations. E) Average sequencing depth per window relative to the mean depth for the entire chromosome. Relative depths were averaged for all individuals in each population. See Figure S14 for whole-genome analysis of the same statistics.

755 To confirm the patterns described above were not driven by genome assembly issues, we
756 also examined the normalized depth of sequencing coverage relative to the chromosome
757 average and discovered a region of variable coverage that overlaps the region of high F_{ST}
758 between Florida and Virginia and is immediately adjacent to the region with zero divergence
759 between Florida and Virginia (Figure 6E, Figure S13). This region (~600kb-700kb) has low
760 coverage in Africa. In Florida and Virginia coverage varies from 0.5X -1X throughout the
761 region. *smoove* identified paired-end evidence for a 52 kb duplication in this region, but
762 genotype calls showed frequencies were similar in Virginia, Florida, and Africa. Combined with
763 the sequencing depth data, these findings suggest copy number variation of these loci might
764 contribute to the Florida-Virginia divergence, though long-read sequencing will likely be
765 required to resolve the sequence variation. The region of elevated F_{ST} between Florida and
766 Virginia and variable copy number contains several genes with neuronal and metabolic
767 functions, offering exciting possibilities for future studies of the potential functional basis of this
768 geographic divergence.

769
770 For comparison, we also examined the same five population signals genome-wide
771 (Figure S14) and observed that the X chromosome is an outlier in many regards. Divergence
772 between Africa and North American samples is greater on the X chromosome (Figure S14A).
773 As previously described (Comeault et al. 2020; Comeault et al. 2021), the X chromosome has
774 reduced genetic diversity relative to autosomes, especially in invaded populations (Figure
775 S14B-C). Tajima's D is negative across the genome for African flies and mostly positive in
776 North American autosomes, indicative of a strong bottleneck in North American flies. However,
777 Tajima's D fluctuates between strongly positive and strongly negative in North American
778 populations along the X chromosome (Figure S14D). This finding, combined with complex
779 patterns of genetic ancestry on the X (Figure 2) and many regions with high haplotype
780 homozygosity (Figure 4), suggest complex evolutionary dynamics on the X that warrant further
781 investigation. These findings agree with Comeault et al. 2021, who found that regions under
782 selection on the X chromosome typically showed higher divergence between invasive
783 populations and African populations. Further global sampling and sequencing of X
784 chromosomes with long reads to resolve inversion genotypes and CNVs may offer insight
785 towards the role of X-linked genes in fueling the ongoing invasion of *Z. indianus*.

786
787

788 **Conclusions**

789

790 In addition to posing economic, health, and environmental threats, invasive species also
791 serve as outstanding models for studying rapid evolution in new environments. Here we report
792 an improved genome assembly and annotation for *Z. indianus*, an introduced drosophilid that
793 is thought to repeatedly recolonize temperate environments each year and is a potential crop
794 pest. We use it for a preliminary assessment of potential rapid evolution and genetic variation
795 in the early stages of invasion. We show that recolonization is likely a stochastic process
796 resulting in different evolutionary dynamics in different years, even within a single orchard. This
797 finding demonstrates broad sampling is important for invasive species that are repeatedly

798 introduced or have multiple introduced populations that may undergo different evolutionary
799 trajectories in different years or different locations. While some founding populations may be
800 small, several population genetic patterns we observe could be explained by ongoing gene
801 flow with the source population, or between temperate populations following recolonization,
802 suggesting gene flow that spreads and maintains favorable alleles could be an important
803 component in *Z. indianus*'s widespread success, as it is for many invasive species (Díez-del-
804 Molino et al. 2013; Medley et al. 2015; Arredondo et al. 2018). Demographic simulations and
805 additional whole genome data will be required to better describe the recent histories of and
806 potential gene flow between invasive populations and to infer colonization routes within North
807 America.

808
809 Though we find limited population structure across space or time in introduced North
810 American populations, we find a region on the X chromosome that may have experienced a
811 selective sweep in North America followed by separate sweeps in Virginia and Florida.
812 Studying how genetic variation in this region of the genome influences survival in temperate
813 environments will be an important direction of future research. We additionally find that the X
814 chromosome has an unusually complex evolutionary history in *Z. indianus*. It may have several
815 segregating inversions and CNVs, has strong signatures of selection, and shows regions of
816 high divergence both between African and North American populations and within North
817 America. Specifically, long-read sequencing strategies will be important to understand likely
818 inversions both on the X and throughout the *Z. indianus* genome that are common in the
819 invaded range. Large inversions can link together adaptive alleles and are often important
820 drivers of evolution in rapidly changing environments (Thompson and Jiggins 2014), so these
821 regions will be important to track over larger spatial and temporal scales in future studies.

822
823 These results underscore the complexity of genetic dynamics during invasions and the
824 need for further studies to explore the adaptive potential and ecological impacts of *Z. indianus*
825 in its invasive range. *Z. indianus* provides a unique system in which we can study independent
826 invasion events across multiple years and locations. One limitation of our study is sample size
827 for each year and location: our ability to estimate allele frequencies or detect subtle changes in
828 allele frequencies across time or space is limited. Sampling strategies that incorporate more
829 individuals, such as pooled sequencing (Bergland et al. 2014; Kapun et al. 2021; Machado et
830 al. 2021; Nunez et al. 2024), will be required to detect these more subtle changes, if they
831 occur, and to understand how they may contribute to rapid adaptation to new environments.
832 The recurrent nature of *Z. indianus* colonization may also offer insight towards the predictability
833 of rapid evolution of invasive species.

834 835 **Data Availability**

836
837 New individual sequencing data has been deposited in the SRA under project number #
838 PRJNA991922. RNA sequencing from larval and pupal samples, and larval Hi-C data used for
839 scaffolding are deposited under the same project number. The genome sequence has been
840 deposited at DDBJ/ENA/GenBank under the accession JAUZU000000000. The metadata for

841 all sequencing samples (including date and location of collection); the annotation information
842 for transcripts, proteins and repeats; and VCFs of SNPs and structural variants have been
843 deposited to Dryad: <https://doi.org/10.5061/dryad.q2bvq83v3>. All code to reproduce analyses
844 has been deposited to Zenodo via Dryad. All code for analysis is also available at:
845 https://github.com/ericksonp/Z.indianus_individual_sequencing/tree/main

846
847 Temporary reviewer dryad link:

848 <http://datadryad.org/stash/share/6td1mtLMrbgLL6lqyaEtpmqK4cigV0VI2Hhqw9Aspvo>

849

850 **Acknowledgments**

851

852 The authors acknowledge The University of Richmond's High Performance Computer
853 (<https://data.richmond.edu/About-HPC-at-UR/index.html>) for providing computational
854 resources that contributed to the results reported herein. We particularly thank George
855 Flanagan for technical support. Preliminary analyses were conducted using resources provided
856 by Research Computing at The University of Virginia (<https://rc.virginia.edu>). We thank the
857 owners and managers of Carter Mountain Orchard and Hanover Peach Orchard for graciously
858 allowing us to collect flies on their properties.

859

860 **Funding**

861

862 This work was funded by award #61-1673 from the Jane Coffin Childs Memorial Fund for
863 Medical Research (to PAE), NIH NIGMS award # R15GM146208 (to PAE), NSF BIO-DEB
864 (EP) award # 2145688 (to AOB), NIH NIGMS award # R35GM119686 (to AOB), and startup
865 funds from the University of Richmond to PAE.

866

867 **Author contributions**

868

869 PAE, AB, AOB: conceptualization; PAE, AOB: funding; PAE, AG: investigation; PAE, AB, NP:
870 resources; PAE: methodology, formal analysis, visualization, writing-original draft; PAE, AOB:
871 writing-reviewing and editing

872

873

874 **References**

875

876 Alexander DH, Lange K. 2011. Enhancements to the ADMIXTURE algorithm for individual
877 ancestry estimation. *BMC Bioinformatics* [Internet] 12:246. Available from:
878 <https://doi.org/10.1186/1471-2105-12-246>

879 Allori Stazzonelli E, Funes CF, Corral Gonzalez MN, Gibilisco SM, Kirschbaum DS. 2023.
880 Population fluctuation and infestation levels of *Zaprionus indianus* Gupta (Diptera:
881 Drosophilidae) in berry crops of northwestern Argentina | International Society for
882 Horticultural Science. *Acta Horticultura* [Internet]. Available from:
883 http://www.actahort.org/books/1381/1381_19.htm

884 Altizer S, Ostfeld RS, Johnson PTJ, Kutz S, Harvell CD. 2013. Climate Change and Infectious
885 Diseases: From Evidence to a Predictive Framework. *Science* 341:514–519.

886 Ananina G, Rohde C, David JR, Valente VLS, Klaczko LB. 2007. Inversion polymorphism and
887 a new polytene chromosome map of *Zaprionus indianus* Gupta (1970) (Diptera:
888 Drosophilidae). *Genetica* 131:117–125.

889 Araripe LO, Klaczko LB, Moreteau B, David JR. 2004. Male sterility thresholds in a tropical
890 cosmopolitan drosophilid, *Zaprionus indianus*. *Journal of Thermal Biology* [Internet]
891 29:73–80. Available from:
892 <http://www.sciencedirect.com/science/article/pii/S0306456503000950>

893 Arredondo TM, Marchini GL, Cruzan MB. 2018. Evidence for human-mediated range
894 expansion and gene flow in an invasive grass. *Proceedings of the Royal Society B:
895 Biological Sciences* [Internet] 285:20181125. Available from:
896 <https://royalsocietypublishing.org/doi/full/10.1098/rspb.2018.1125>

897 Atsawawaranunt K, Ewart KM, Major RE, Johnson RN, Santure AW, Whibley A. 2023. Tracing
898 the introduction of the invasive common myna using population genomics. *Heredity*
899 [Internet] 131:56–67. Available from: [https://www.nature.com/articles/s41437-023-](https://www.nature.com/articles/s41437-023-00621-w)
900 [00621-w](https://www.nature.com/articles/s41437-023-00621-w)

901 Avalos A, Pan H, Li C, Acevedo-Gonzalez JP, Rendon G, Fields CJ, Brown PJ, Giray T,
902 Robinson GE, Hudson ME, et al. 2017. A soft selective sweep during rapid evolution of
903 gentle behaviour in an Africanized honeybee. *Nat Commun* [Internet] 8:1550. Available
904 from: <https://www.nature.com/articles/s41467-017-01800-0>

905 Bao Z, Eddy SR. 2002. Automated De Novo Identification of Repeat Sequence Families in
906 Sequenced Genomes. *Genome Res.* [Internet] 12:1269–1276. Available from:
907 <https://genome.cshlp.org/content/12/8/1269>

908 Barrett CF, Corbett CW, Thixton-Nolan HL. 2023. A lack of population structure characterizes
909 the invasive *Lonicera japonica* in West Virginia and across eastern North America^{1,2}.
910 *tbot* [Internet] 150:455–466. Available from: [https://bioone.org/journals/the-journal-of-](https://bioone.org/journals/the-journal-of-the-torrey-botanical-society/volume-150/issue-3/TORREY-D-23-00007.1/A-lack-of-population-structure-characterizes-the-invasive-Lonicera-japonica/10.3159/TORREY-D-23-00007.1.full)
911 [the-torrey-botanical-society/volume-150/issue-3/TORREY-D-23-00007.1/A-lack-of-](https://bioone.org/journals/the-torrey-botanical-society/volume-150/issue-3/TORREY-D-23-00007.1/A-lack-of-population-structure-characterizes-the-invasive-Lonicera-japonica/10.3159/TORREY-D-23-00007.1.full)
912 [population-structure-characterizes-the-invasive-Lonicera-japonica/10.3159/TORREY-D-](https://bioone.org/journals/the-torrey-botanical-society/volume-150/issue-3/TORREY-D-23-00007.1/A-lack-of-population-structure-characterizes-the-invasive-Lonicera-japonica/10.3159/TORREY-D-23-00007.1.full)
913 [23-00007.1.full](https://bioone.org/journals/the-torrey-botanical-society/volume-150/issue-3/TORREY-D-23-00007.1/A-lack-of-population-structure-characterizes-the-invasive-Lonicera-japonica/10.3159/TORREY-D-23-00007.1.full)

- 914 Barrett RDH, Laurent S, Mallarino R, Pfeifer SP, Xu CCY, Foll M, Wakamatsu K, Duke-Cohan
915 JS, Jensen JD, Hoekstra HE. 2019. Linking a mutation to survival in wild mice. *Science*
916 363:499–504.
- 917 Barrett SCH. 2015. Foundations of invasion genetics: the Baker and Stebbins legacy.
918 *Molecular Ecology* [Internet] 24:1927–1941. Available from:
919 <https://onlinelibrary.wiley.com/doi/abs/10.1111/mec.13014>
- 920 Bellard C, Bertelsmeier C, Leadley P, Thuiller W, Courchamp F. 2012. Impacts of climate
921 change on the future of biodiversity. *Ecology Letters* 15:365–377.
- 922 Bemmels JB, Mikkelsen EK, Haddrath O, Colbourne RM, Robertson HA, Weir JT. 2021.
923 Demographic decline and lineage-specific adaptations characterize New Zealand kiwi.
924 *Proc Biol Sci* 288:20212362.
- 925 Bergland AO, Behrman EL, O'Brien KR, Schmidt PS, Petrov DA. 2014. Genomic Evidence of
926 Rapid and Stable Adaptive Oscillations over Seasonal Time Scales in *Drosophila*. *PLoS*
927 *Genet* [Internet] 10:e1004775. Available from:
928 <http://dx.doi.org/10.1371/journal.pgen.1004775>
- 929 Bushnell B, Rood J, Singer E. 2017. BBMerge – Accurate paired shotgun read merging via
930 overlap. *PLOS ONE* 12:e0185056.
- 931 Cabanettes F, Klopp C. 2018. D-GENIES: dot plot large genomes in an interactive, efficient
932 and simple way. *PeerJ* [Internet] 6:e4958. Available from: <https://peerj.com/articles/4958>
- 933 Campos SRC, Rieger TT, Santos JF. 2007. Homology of polytene elements between
934 *Drosophila* and *Zaprionus* determined by in situ hybridization in *Zaprionus indianus*.
935 *Genet Mol Res* 6:262–276.
- 936 Cantarel BL, Korf I, Robb SMC, Parra G, Ross E, Moore B, Holt C, Alvarado AS, Yandell M.
937 2008. MAKER: An easy-to-use annotation pipeline designed for emerging model
938 organism genomes. *Genome Res.* [Internet] 18:188–196. Available from:
939 <https://genome.cshlp.org/content/18/1/188>
- 940 Chan PP, Lowe TM. 2019. tRNAscan-SE: Searching for tRNA genes in genomic sequences.
941 *Methods Mol Biol* [Internet] 1962:1–14. Available from:
942 <https://www.ncbi.nlm.nih.gov/pmc/articles/PMC6768409/>
- 943 Chang CC, Chow CC, Tellier LC, Vattikuti S, Purcell SM, Lee JJ. 2015. Second-generation
944 PLINK: rising to the challenge of larger and richer datasets. *Gigascience* 4:7.
- 945 Clements DR, Ditommaso A. 2011. Climate change and weed adaptation: can evolution of
946 invasive plants lead to greater range expansion than forecasted? *Weed Research*
947 51:227–240.
- 948 Comeault AA, Kautt AF, Matute DR. 2021. Genomic signatures of admixture and selection are
949 shared among populations of *Zaprionus indianus* across the western hemisphere.
950 *Molecular Ecology* 30:6193–6210.

- 951 Comeault AA, Wang J, Tittes S, Isbell K, Ingley S, Hurlbert AH, Matute DR. 2020. Genetic
952 Diversity and Thermal Performance in Invasive and Native Populations of African Fig
953 Flies. *Molecular Biology and Evolution* 37:1893–1906.
- 954 Commar LS, Galego LG da C, Ceron CR, Carareto CMA. 2012. Taxonomic and evolutionary
955 analysis of *Zaprionus indianus* and its colonization of Palearctic and Neotropical
956 regions. *Genet Mol Biol* 35:395–406.
- 957 Danecek P, Auton A, Abecasis G, Albers CA, Banks E, DePristo MA, Handsaker RE, Lunter G,
958 Marth GT, Sherry ST, et al. 2011. The variant call format and VCFtools. *Bioinformatics*
959 [Internet] 27:2156–2158. Available from: <https://doi.org/10.1093/bioinformatics/btr330>
- 960 Danecek P, Bonfield JK, Liddle J, Marshall J, Ohan V, Pollard MO, Whitwham A, Keane T,
961 McCarthy SA, Davies RM, et al. 2021. Twelve years of SAMtools and BCFtools.
962 *Gigascience* 10:giab008.
- 963 Díez-del-Molino D, Carmona-Catot G, Araguas R-M, Vidal O, Sanz N, García-Berthou E,
964 García-Marín J-L. 2013. Gene Flow and Maintenance of Genetic Diversity in Invasive
965 Mosquitofish (*Gambusia holbrooki*). *PLOS ONE* [Internet] 8:e82501. Available from:
966 <https://journals.plos.org/plosone/article?id=10.1371/journal.pone.0082501>
- 967 Dobin A, Davis CA, Schlesinger F, Drenkow J, Zaleski C, Jha S, Batut P, Chaisson M,
968 Gingeras TR. 2013. STAR: ultrafast universal RNA-seq aligner. *Bioinformatics* [Internet]
969 29:15–21. Available from: <https://www.ncbi.nlm.nih.gov/pmc/articles/PMC3530905/>
- 970 Dowle M, Srinivasan A. 2019. data.table: Extension of `data.frame`. Available from:
971 <https://CRAN.R-project.org/package=data.table>
- 972 Ellegren H. 2009. The different levels of genetic diversity in sex chromosomes and autosomes.
973 *Trends in Genetics* [Internet] 25:278–284. Available from:
974 <https://www.sciencedirect.com/science/article/pii/S0168952509000900>
- 975 Ellstrand NC, Schierenbeck KA. 2000. Hybridization as a stimulus for the evolution of
976 invasiveness in plants? *Proceedings of the National Academy of Sciences* [Internet]
977 97:7043–7050. Available from: <https://www.pnas.org/doi/abs/10.1073/pnas.97.13.7043>
- 978 Erickson PA, Weller CA, Song DY, Bangerter AS, Schmidt P, Bergland AO. 2020. Unique
979 genetic signatures of local adaptation over space and time for diapause, an ecologically
980 relevant complex trait, in *Drosophila melanogaster*. *PLOS Genetics* 16:e1009110.
- 981 Estoup A, Ravigné V, Hufbauer R, Vitalis R, Gautier M, Facon B. 2016. Is There a Genetic
982 Paradox of Biological Invasion? [https://doi.org/10.1146/annurev-ecolsys-121415-](https://doi.org/10.1146/annurev-ecolsys-121415-032116)
983 [032116](https://doi.org/10.1146/annurev-ecolsys-121415-032116) [Internet]. Available from:
984 <https://www.annualreviews.org/doi/abs/10.1146/annurev-ecolsys-121415-032116>
- 985 Fang Z, Pyhäjärvi T, Weber AL, Dawe RK, Glaubitz JC, González J de JS, Ross-Ibarra C,
986 Doebley J, Morrell PL, Ross-Ibarra J. 2012. Megabase-Scale Inversion Polymorphism in
987 the Wild Ancestor of Maize. *Genetics* [Internet] 191:883–894. Available from:
988 <https://doi.org/10.1534/genetics.112.138578>

- 989 Feron R, Waterhouse RM. 2022. Assessing species coverage and assembly quality of rapidly
990 accumulating sequenced genomes. *GigaScience* [Internet] 11:giac006. Available from:
991 <https://doi.org/10.1093/gigascience/giac006>
- 992 Flynn JM, Hubley R, Goubert C, Rosen J, Clark AG, Feschotte C, Smit AF. 2020.
993 RepeatModeler2 for automated genomic discovery of transposable element families.
994 *Proceedings of the National Academy of Sciences* [Internet] 117:9451–9457. Available
995 from: <https://www.pnas.org/doi/full/10.1073/pnas.1921046117>
- 996 Fournier D, Aron S. 2021. Hybridization and invasiveness in social insects — The good, the
997 bad and the hybrid. *Current Opinion in Insect Science* [Internet] 46:1–9. Available from:
998 <https://www.sciencedirect.com/science/article/pii/S2214574521000018>
- 999 Friedline CJ, Faske TM, Lind BM, Hobson EM, Parry D, Dyer RJ, Johnson DM, Thompson LM,
1000 Grayson KL, Eckert AJ. 2019. Evolutionary genomics of gypsy moth populations
1001 sampled along a latitudinal gradient. *Molecular Ecology* [Internet] 0. Available from:
1002 <https://onlinelibrary.wiley.com/doi/abs/10.1111/mec.15069>
- 1003 Galludo M, Canals J, Pineda-Cirera L, Esteve C, Rosselló M, Balanyà J, Arenas C, Mestres F.
1004 2018. Climatic adaptation of chromosomal inversions in *Drosophila subobscura*.
1005 *Genetica* [Internet] 146:433–441. Available from: [https://doi.org/10.1007/s10709-018-](https://doi.org/10.1007/s10709-018-0035-x)
1006 0035-x
- 1007 García-Escudero CA, Tsigenopoulos CS, Manousaki T, Tsakogiannis A, Marbà N, Vizzini S,
1008 Duarte CM, Apostolaki ET. 2023. Population genomics unveils the century-old invasion
1009 of the Seagrass *Halophila stipulacea* in the Mediterranean Sea. *Mar Biol* [Internet]
1010 171:40. Available from: <https://doi.org/10.1007/s00227-023-04361-7>
- 1011 Garnier S. 2018. viridis: Default Color Maps from “matplotlib.” Available from: [https://CRAN.R-](https://CRAN.R-project.org/package=viridis)
1012 project.org/package=viridis
- 1013 Garud NR, Messer PW, Buzbas EO, Petrov DA. 2015. Recent Selective Sweeps in North
1014 American *Drosophila melanogaster* Show Signatures of Soft Sweeps. *PLOS Genetics*
1015 [Internet] 11:e1005004. Available from:
1016 <https://journals.plos.org/plosgenetics/article?id=10.1371/journal.pgen.1005004>
- 1017 Gautier M, Vitalis R. 2012. rehh: an R package to detect footprints of selection in genome-wide
1018 SNP data from haplotype structure. *Bioinformatics* 28:1176–1177.
- 1019 Gleason JM, Roy PR, Everman ER, Gleason TC, Morgan TJ. 2019. Phenology of *Drosophila*
1020 species across a temperate growing season and implications for behavior. *PLOS ONE*
1021 14:e0216601.
- 1022 Good BH, McDonald MJ, Barrick JE, Lenski RE, Desai MM. 2017. The dynamics of molecular
1023 evolution over 60,000 generations. *Nature* 551:45–50.
- 1024 Gupta JP. 1970. Description of a new species of *Phorticella zaprionus* (Drosophilidae) from
1025 India. *Proceedings of the Indian National Science Academy* 36B:62–70.
- 1026 Gupta JP, Kumar A. 1987. Cytogenetics of *Zaprionus indianus* Gupta (Diptera: Drosophilidae):
1027 Nucleolar organizer regions, mitotic and polytene chromosomes and inversion

- 1028 polymorphism. *Genetica* [Internet] 74:19–25. Available from:
1029 <https://doi.org/10.1007/BF00055090>
- 1030 Hancock AM, Brachi B, Faure N, Horton MW, Jarymowycz LB, Sperone FG, Toomajian C,
1031 Roux F, Bergelson J. 2011. Adaptation to Climate Across the *Arabidopsis thaliana*
1032 Genome. *Science* 334:83–86.
- 1033 Hoberg EP, Brooks DR. 2015. Evolution in action: climate change, biodiversity dynamics and
1034 emerging infectious disease. *Philosophical Transactions of the Royal Society B:*
1035 *Biological Sciences* 370:20130553.
- 1036 Holle SG, Tran AK, Burkness EC, Ebbenga DN, Hutchison WD. 2018. First Detections of
1037 *Zaprionus indianus* (Diptera: Drosophilidae) in Minnesota. *ents* 54:99–102.
- 1038 Huang K, Andrew RL, Owens GL, Ostevik KL, Rieseberg LH. 2020. Multiple chromosomal
1039 inversions contribute to adaptive divergence of a dune sunflower ecotype. *Molecular*
1040 *Ecology* [Internet] 29:2535–2549. Available from:
1041 <https://onlinelibrary.wiley.com/doi/abs/10.1111/mec.15428>
- 1042 Johnson MS, Gopalakrishnan S, Goyal J, Dillingham ME, Bakerlee CW, Humphrey PT,
1043 Jagdish T, Jerison ER, Kosheleva K, Lawrence KR, et al. 2021. Phenotypic and
1044 molecular evolution across 10,000 generations in laboratory budding yeast
1045 populations. Verstrepen KJ, Wittkopp PJ, Verstrepen KJ, Hodgins-Davis A, editors. *eLife*
1046 10:e63910.
- 1047 Jones MR, Mills LS, Alves PC, Callahan CM, Alves JM, Lafferty DJR, Jiggins FM, Jensen JD,
1048 Melo-Ferreira J, Good JM. 2018. Adaptive introgression underlies polymorphic seasonal
1049 camouflage in snowshoe hares. *Science* 360:1355–1358.
- 1050 Joron M, Frezal L, Jones RT, Chamberlain NL, Lee SF, Haag CR, Whibley A, Becuwe M,
1051 Baxter SW, Ferguson L, et al. 2011. Chromosomal rearrangements maintain a
1052 polymorphic supergene controlling butterfly mimicry. *Nature* [Internet] 477:203–206.
1053 Available from: <http://www.nature.com/nature/journal/v477/n7363/full/nature10341.html>
- 1054 Joshi NK, Biddinger DJ, Demchak K, Deppen A. 2014. First report of *Zaprionus indianus*
1055 (Diptera: Drosophilidae) in commercial fruits and vegetables in Pennsylvania. *J. Insect*
1056 *Sci.* 14:259.
- 1057 Kapun M, Nunez JCB, Bogaerts-Márquez M, Murga-Moreno J, Paris M, Outten J, Coronado-
1058 Zamora M, Tern C, Rota-Stabelli O, Guerreiro MPG, et al. 2021. *Drosophila* Evolution
1059 over Space and Time (DEST) - A New Population Genomics Resource. *bioRxiv*
1060 [Internet]:2021.02.01.428994. Available from:
1061 <https://www.biorxiv.org/content/10.1101/2021.02.01.428994v1>
- 1062 Keller O, Kollmar M, Stanke M, Waack S. 2011. A novel hybrid gene prediction method
1063 employing protein multiple sequence alignments. *Bioinformatics* [Internet] 27:757–763.
1064 Available from: <https://doi.org/10.1093/bioinformatics/btr010>
- 1065 Kim BY, Wang JR, Miller DE, Barmina O, Delaney E, Thompson A, Comeault AA, Peede D,
1066 D’Agostino ER, Pelaez J, et al. 2021. Highly contiguous assemblies of 101 drosophilid

- 1067 genomes.Coop G, Wittkopp PJ, Sackton TB, editors. *eLife* [Internet] 10:e66405.
1068 Available from: <https://doi.org/10.7554/eLife.66405>
- 1069 Koch JB, Dupuis JR, Jardeleza M-K, Ouedraogo N, Geib SM, Follett PA, Price DK. 2020.
1070 Population genomic and phenotype diversity of invasive *Drosophila suzukii* in Hawai'i.
1071 *Biol Invasions* [Internet] 22:1753–1770. Available from: [https://doi.org/10.1007/s10530-](https://doi.org/10.1007/s10530-020-02217-5)
1072 020-02217-5
- 1073 Korf I. 2004. Gene finding in novel genomes. *BMC Bioinformatics* [Internet] 5:59. Available
1074 from: <https://doi.org/10.1186/1471-2105-5-59>
- 1075 Korneliussen TS, Albrechtsen A, Nielsen R. 2014. ANGSD: Analysis of Next Generation
1076 Sequencing Data. *BMC Bioinformatics* [Internet] 15:356. Available from:
1077 <https://doi.org/10.1186/s12859-014-0356-4>
- 1078 Korunes KL, Samuk K. 2021. pixy: Unbiased estimation of nucleotide diversity and divergence
1079 in the presence of missing data. *Molecular Ecology Resources* [Internet] 21:1359–1368.
1080 Available from: <https://onlinelibrary.wiley.com/doi/abs/10.1111/1755-0998.13326>
- 1081 Kremmer L, David J, Borowiec N, Thaon M, Ris N, Poirie M, Gatti J-L. 2017. The African fig fly
1082 *Zaprionus indianus*: a new invasive pest in France? *Bulletin of Insectology* 70:57–62.
- 1083 Küpper C, Stocks M, Risse JE, dos Remedios N, Farrell LL, McRae SB, Morgan TC,
1084 Karlionova N, Pinchuk P, Verkuil YI, et al. 2016. A supergene determines highly
1085 divergent male reproductive morphs in the ruff. *Nat Genet* [Internet] 48:79–83. Available
1086 from: <http://www.nature.com/ng/journal/v48/n1/full/ng.3443.html>
- 1087 Leão BFD, Tidon R. 2004. Newly invading species exploiting native host-plants: the case of
1088 the African *Zaprionus indianus* (Gupta) in the Brazilian Cerrado (Diptera,
1089 *Drosophilidae*). *Annales de la Société entomologique de France (N.S.)* 40:285–290.
- 1090 Lee YW, Fishman L, Kelly JK, Willis JH. 2016. A Segregating Inversion Generates Fitness
1091 Variation in Yellow Monkeyflower (*Mimulus guttatus*). *Genetics* [Internet] 202:1473–
1092 1484. Available from: <http://www.genetics.org/content/202/4/1473>
- 1093 Li H, Durbin R. 2009. Fast and accurate short read alignment with Burrows-Wheeler transform.
1094 *Bioinformatics* 25:1754–1760.
- 1095 Li H, Handsaker B, Wysoker A, Fennell T, Ruan J, Homer N, Marth G, Abecasis G, Durbin R,
1096 1000 Genome Project Data Processing Subgroup. 2009. The Sequence Alignment/Map
1097 format and SAMtools. *Bioinformatics* [Internet] 25:2078–2079. Available from:
1098 <https://doi.org/10.1093/bioinformatics/btp352>
- 1099 Li H, Peng Y, Wang Y, Summerhays B, Shu X, Vasquez Y, Vansant H, Grenier C, Gonzalez N,
1100 Kansagra K, et al. 2023. Global patterns of genomic and phenotypic variation in the
1101 invasive harlequin ladybird. *BMC Biol* [Internet] 21:141. Available from:
1102 <https://doi.org/10.1186/s12915-023-01638-7>
- 1103 Li H, Ralph P. 2019. Local PCA Shows How the Effect of Population Structure Differs Along
1104 the Genome. *Genetics* [Internet] 211:289–304. Available from:
1105 <https://www.ncbi.nlm.nih.gov/pmc/articles/PMC6325702/>

- 1106 Linde K van der, Steck GJ, Hibbard K, Birdsley JS, Alonso LM, Houle D. 2006. FIRST
1107 RECORDS OF ZAPRIONUS INDIANUS (DIPTERA: DROSOPHILIDAE), A PEST
1108 SPECIES ON COMMERCIAL FRUITS FROM PANAMA AND THE UNITED STATES
1109 OF AMERICA. *flen* 89:402–404.
- 1110 Lovell JT, MacQueen AH, Mamidi S, Bonnette J, Jenkins J, Napier JD, Sreedasyam A, Healey
1111 A, Session A, Shu S, et al. 2021. Genomic mechanisms of climate adaptation in
1112 polyploid bioenergy switchgrass. *Nature*:1–7.
- 1113 Ma L, Cao L-J, Hoffmann AA, Gong Y-J, Chen J-C, Chen H-S, Wang X-B, Zeng A-P, Wei S-J,
1114 Zhou Z-S. 2020. Rapid and strong population genetic differentiation and genomic
1115 signatures of climatic adaptation in an invasive mealybug. *Diversity and Distributions*
1116 [Internet] 26:610–622. Available from:
1117 <https://onlinelibrary.wiley.com/doi/abs/10.1111/ddi.13053>
- 1118 Ma L-J, Cao L-J, Chen J-C, Tang M-Q, Song W, Yang F-Y, Shen X-J, Ren Y-J, Yang Q, Li H,
1119 et al. 2024. Rapid and Repeated Climate Adaptation Involving Chromosome Inversions
1120 following Invasion of an Insect. *Molecular Biology and Evolution* [Internet] 41:msae044.
1121 Available from: <https://doi.org/10.1093/molbev/msae044>
- 1122 Machado HE, Bergland AO, Taylor R, Tilk S, Behrman E, Dyer K, Fabian DK, Flatt T,
1123 González J, Karasov TL, et al. 2021. Broad geographic sampling reveals the shared
1124 basis and environmental correlates of seasonal adaptation in *Drosophila*. Nordborg M,
1125 Wittkopp PJ, Nordborg M, editors. *eLife* [Internet] 10:e67577. Available from:
1126 <https://doi.org/10.7554/eLife.67577>
- 1127 Manni M, Berkeley MR, Seppey M, Simão FA, Zdobnov EM. 2021. BUSCO Update: Novel and
1128 Streamlined Workflows along with Broader and Deeper Phylogenetic Coverage for
1129 Scoring of Eukaryotic, Prokaryotic, and Viral Genomes. *Molecular Biology and Evolution*
1130 [Internet] 38:4647–4654. Available from: <https://doi.org/10.1093/molbev/msab199>
- 1131 Markow TA, Hanna G, Riesgo-Escovar JR, Tellez-Garcia AA, Richmond MP, Nazario-Yepiz
1132 NO, Laclette MRL, Carpinteyro-Ponce J, Pfeiler E. 2014. Population genetics and
1133 recent colonization history of the invasive drosophilid *Zaprionus indianus* in Mexico and
1134 Central America. *Biol Invasions* 16:2427–2434.
- 1135 da Mata RA, Tidon R, Côrtes LG, De Marco P, Diniz-Filho JAF. 2010. Invasive and flexible:
1136 niche shift in the drosophilid *Zaprionus indianus* (Insecta, Diptera). *Biol Invasions*
1137 12:1231–1241.
- 1138 Matheson P, McGaughran A. 2022. Genomic data is missing for many highly invasive species,
1139 restricting our preparedness for escalating incursion rates. *Sci Rep* [Internet] 12:13987.
1140 Available from: <https://www.nature.com/articles/s41598-022-17937-y>
- 1141 McGaughran A, Dhimi MK, Parvizi E, Vaughan AL, Gleeson DM, Hodgins KA, Rollins LA,
1142 Tepolt CK, Turner KG, Atsawawaranunt K, et al. 2024. Genomic Tools in Biological
1143 Invasions: Current State and Future Frontiers. *Genome Biology and Evolution* [Internet]
1144 16:evad230. Available from: <https://doi.org/10.1093/gbe/evad230>

- 1145 McKenna A, Hanna M, Banks E, Sivachenko A, Cibulskis K, Kernytsky A, Garimella K,
1146 Altshuler D, Gabriel S, Daly M, et al. 2010. The Genome Analysis Toolkit: a MapReduce
1147 framework for analyzing next-generation DNA sequencing data. *Genome Res.*
1148 20:1297–1303.
- 1149 Medley KA, Jenkins DG, Hoffman EA. 2015. Human-aided and natural dispersal drive gene
1150 flow across the range of an invasive mosquito. *Molecular Ecology* [Internet] 24:284–
1151 295. Available from: <https://onlinelibrary.wiley.com/doi/abs/10.1111/mec.12925>
- 1152 Messer PW, Petrov DA. 2013. Population genomics of rapid adaptation by soft selective
1153 sweeps. *Trends in Ecology & Evolution* [Internet] 28:659–669. Available from:
1154 [https://www.cell.com/trends/ecology-evolution/abstract/S0169-5347\(13\)00207-3](https://www.cell.com/trends/ecology-evolution/abstract/S0169-5347(13)00207-3)
- 1155 Microsoft, Weston S. 2017. foreach: Provides Foreach Looping Construct for R. Available
1156 from: <https://CRAN.R-project.org/package=foreach>
- 1157 Nava DE, Nascimento AM, Stein CP, Haddad ML, Bento JMS, Parra JRP. 2007. Biology,
1158 thermal requirements, and estimation of the number of generations of *Zaprionus*
1159 *indianus* (Diptera: Drosophilidae) for the main fig producing regions of Brazil. *flen*
1160 90:495–501.
- 1161 Nguyen Ba AN, Cvijović I, Rojas Echenique JI, Lawrence KR, Rego-Costa A, Liu X, Levy SF,
1162 Desai MM. 2019. High-resolution lineage tracking reveals travelling wave of adaptation
1163 in laboratory yeast. *Nature* 575:494–499.
- 1164 Nowling RJ, Manke KR, Emrich SJ. 2020. Detecting inversions with PCA in the presence of
1165 population structure. *PLOS ONE* [Internet] 15:e0240429. Available from:
1166 <https://journals.plos.org/plosone/article?id=10.1371/journal.pone.0240429>
- 1167 Nunez JCB, Lenhart BA, Bangerter A, Murray CS, Mazzeo GR, Yu Y, Nystrom TL, Tern C,
1168 Erickson PA, Bergland AO. 2024. A cosmopolitan inversion facilitates seasonal
1169 adaptation in overwintering *Drosophila*. *Genetics* [Internet] 226:iyad207. Available from:
1170 <https://doi.org/10.1093/genetics/iyad207>
- 1171 Oerke E-C. 2006. Crop losses to pests. *The Journal of Agricultural Science* 144:31–43.
- 1172 Oliveira CM, Auad AM, Mendes SM, Frizzas MR. 2013. Economic impact of exotic insect pests
1173 in Brazilian agriculture. *Journal of Applied Entomology* 137:1–15.
- 1174 Parchami-Araghi M, Gilasian E, Keyhanian A. 2015. Olive infestation with *Zaprionus indianus*
1175 Gupta (Dip.: Drosophilidae) in northern Iran: a new host record and threat to world olive
1176 production. *Drosophila Information Service* 98:60–61.
- 1177 Parvizi E, Dhami MK, Yan J, McGaughan A. 2023. Population genomic insights into invasion
1178 success in a polyphagous agricultural pest, *Halyomorpha halys*. *Molecular Ecology*
1179 [Internet] 32:138–151. Available from:
1180 <https://onlinelibrary.wiley.com/doi/abs/10.1111/mec.16740>
- 1181 Patterson M, Marschall T, Pisanti N, van Iersel L, Stougie L, Klau GW, Schönhuth A. 2015.
1182 WhatsHap: Weighted Haplotype Assembly for Future-Generation Sequencing Reads. *J*
1183 *Comput Biol* 22:498–509.

- 1184 Patton AH, Margres MJ, Stahlke AR, Hendricks S, Lewallen K, Hamede RK, Ruiz-Aravena M,
1185 Ryder O, McCallum HI, Jones ME, et al. 2019. Contemporary Demographic
1186 Reconstruction Methods Are Robust to Genome Assembly Quality: A Case Study in
1187 Tasmanian Devils. *Molecular Biology and Evolution* [Internet] 36:2906–2921. Available
1188 from: <https://doi.org/10.1093/molbev/msz191>
- 1189 Pedersen BS, Layer R, Quinlan AR. 2020. smooove: structural-variant calling and genotyping
1190 with existing tools.
- 1191 Pélissié B, Chen YH, Cohen ZP, Crossley MS, Hawthorne DJ, Izzo V, Schoville SD. 2022.
1192 Genome Resequencing Reveals Rapid, Repeated Evolution in the Colorado Potato
1193 Beetle. *Molecular Biology and Evolution* [Internet] 39:msac016. Available from:
1194 <https://doi.org/10.1093/molbev/msac016>
- 1195 Pfeiffer DG, Shrader ME, Wahls JCE, Willbrand BN, Sandum I, van der Linde K, Laub CA,
1196 Mays RS, Day ER. 2019. African Fig Fly (Diptera: Drosophilidae): Biology, Expansion of
1197 Geographic Range, and Its Potential Status as a Soft Fruit Pest. *J Integr Pest Manag*
1198 [Internet] 10. Available from: <https://academic.oup.com/jipm/article/10/1/20/5514212>
- 1199 Picq S, Wu Y, Martemyanov VV, Pouliot E, Pfister SE, Hamelin R, Cusson M. 2023. Range-
1200 wide population genomics of the spongy moth, *Lymantria dispar* (Erebidae):
1201 Implications for biosurveillance, subspecies classification and phylogeography of a
1202 destructive moth. *Evolutionary Applications* [Internet] 16:638–656. Available from:
1203 <https://onlinelibrary.wiley.com/doi/abs/10.1111/eva.13522>
- 1204 Platts PJ, Mason SC, Palmer G, Hill JK, Oliver TH, Powney GD, Fox R, Thomas CD. 2019.
1205 Habitat availability explains variation in climate-driven range shifts across multiple
1206 taxonomic groups. *Scientific Reports* 9:15039.
- 1207 Price AL, Jones NC, Pevzner PA. 2005. De novo identification of repeat families in large
1208 genomes. *Bioinformatics* [Internet] 21:i351–i358. Available from:
1209 <https://doi.org/10.1093/bioinformatics/bti1018>
- 1210 Purcell S, Neale B, Todd-Brown K, Thomas L, Ferreira MAR, Bender D, Maller J, Sklar P, de
1211 Bakker PIW, Daly MJ, et al. 2007. PLINK: a tool set for whole-genome association and
1212 population-based linkage analyses. *Am. J. Hum. Genet.* 81:559–575.
- 1213 Putnam NH, O’Connell BL, Stites JC, Rice BJ, Blanchette M, Calef R, Troll CJ, Fields A,
1214 Hartley PD, Sugnet CW, et al. 2016. Chromosome-scale shotgun assembly using an in
1215 vitro method for long-range linkage. *Genome Res* [Internet] 26:342–350. Available from:
1216 <https://www.ncbi.nlm.nih.gov/pmc/articles/PMC4772016/>
- 1217 R Core Team. R: A language and environment for statistical computing. Available from:
1218 <http://www.R-project.org/>
- 1219 Rakes LM, Delamont M, Cole C, Yates JA, Blevins LJ, Hassan FN, Bergland AO, Erickson PA.
1220 2023. A small survey of introduced *Zaprionus indianus* (Diptera: Drosophilidae) in
1221 orchards of the eastern United States. *Journal of Insect Science* [Internet] 23:21.
1222 Available from: <https://doi.org/10.1093/jisesa/iead092>

- 1223 Renkema JM, Miller M, Fraser H, Légaré J-P, Hallett RH. 2013. First records of *Zaprionus*
1224 *indianus* Gupta (Diptera: Drosophilidae) from commercial fruit fields in Ontario and
1225 Quebec, Canada. *The Journal of the Entomological Society of Ontario* [Internet] 144.
1226 Available from: <https://journal.lib.uoguelph.ca/index.php/eso/article/view/3745>
- 1227 Ricciardi A. 2007. Are modern biological invasions an unprecedented form of global change?
1228 *Conserv Biol* 21:329–336.
- 1229 Roman G, Meller V, Wu KH, Davis RL. 1998. The opt1 gene of *Drosophila melanogaster*
1230 encodes a proton-dependent dipeptide transporter. *American Journal of Physiology-Cell*
1231 *Physiology* [Internet] 275:C857–C869. Available from:
1232 <https://journals.physiology.org/doi/full/10.1152/ajpcell.1998.275.3.C857>
- 1233 Roque F, Matavelli C, Lopes PHS, Machida WS, Von Zuben CJ, Tidon R. 2017. Brazilian Fig
1234 Plantations Are Dominated by Widely Distributed Drosophilid Species (Diptera:
1235 Drosophilidae). *Annals of the Entomological Society of America* 110:521–527.
- 1236 Sabeti PC, Varilly P, Fry B, Lohmueller J, Hostetter E, Cotsapas C, Xie X, Byrne EH, McCarroll
1237 SA, Gaudet R, et al. 2007. Genome-wide detection and characterization of positive
1238 selection in human populations. *Nature* [Internet] 449:913–918. Available from:
1239 <https://www.ncbi.nlm.nih.gov/pmc/articles/PMC2687721/>
- 1240 Sardain A, Sardain E, Leung B. 2019. Global forecasts of shipping traffic and biological
1241 invasions to 2050. *Nature Sustainability* 2:274–282.
- 1242 Schluter D, Marchinko KB, Arnegard ME, Zhang H, Brady SD, Jones FC, Bell MA, Kingsley
1243 DM. 2021. Fitness maps to a large-effect locus in introduced stickleback populations.
1244 *PNAS* [Internet] 118. Available from: <https://www.pnas.org/content/118/3/e1914889118>
- 1245 Seebens H, Blackburn TM, Dyer EE, Genovesi P, Hulme PE, Jeschke JM, Pagad S, Pyšek P,
1246 Winter M, Arianoutsou M, et al. 2017. No saturation in the accumulation of alien species
1247 worldwide. *Nature Communications* 8:14435.
- 1248 Seebens H, Essl F, Dawson W, Fuentes N, Moser D, Pergl J, Pyšek P, Kleunen M van, Weber
1249 E, Winter M, et al. 2015. Global trade will accelerate plant invasions in emerging
1250 economies under climate change. *Global Change Biology* 21:4128–4140.
- 1251 da Silva VH, Laine VN, Bosse M, Spurgin LG, Derks MFL, van Oers K, Dibbits B, Slate J,
1252 Crooijmans RPMA, Visser ME, et al. 2019. The Genomic Complexity of a Large
1253 Inversion in Great Tits. *Genome Biology and Evolution* [Internet] 11:1870–1881.
1254 Available from: <https://doi.org/10.1093/gbe/evz106>
- 1255 Simão FA, Waterhouse RM, Ioannidis P, Kriventseva EV, Zdobnov EM. 2015. BUSCO:
1256 assessing genome assembly and annotation completeness with single-copy orthologs.
1257 *Bioinformatics* [Internet] 31:3210–3212. Available from:
1258 <https://doi.org/10.1093/bioinformatics/btv351>
- 1259 Smit A, Hubley R, Green P. 2015. RepeatMasker Open-4.0. Available from:
1260 <http://www.repeatmasker.org>

- 1261 Soudi S, Crepeau M, Collier TC, Lee Y, Cornel AJ, Lanzaro GC. 2023. Genomic signatures of
1262 local adaptation in recent invasive *Aedes aegypti* populations in California. *BMC*
1263 *Genomics* [Internet] 24:311. Available from: [https://doi.org/10.1186/s12864-023-09402-](https://doi.org/10.1186/s12864-023-09402-5)
1264 5
- 1265 Steenwyk JL, Rokas A. 2021. ggpubfigs: Colorblind-Friendly Color Palettes and ggplot2
1266 Graphic System Extensions for Publication-Quality Scientific Figures. *Microbiology*
1267 *Resource Announcements* [Internet] 10:10.1128/mra.00871-21. Available from:
1268 <https://journals.asm.org/doi/10.1128/MRA.00871-21>
- 1269 Stern DB, Lee CE. 2020. Evolutionary origins of genomic adaptations in an invasive copepod.
1270 *Nat Ecol Evol* [Internet] 4:1084–1094. Available from:
1271 <https://www.nature.com/articles/s41559-020-1201-y>
- 1272 Stuart KC, Cardilini APA, Cassey P, Richardson MF, Sherwin WB, Rollins LA, Sherman CDH.
1273 2021. Signatures of selection in a recent invasion reveal adaptive divergence in a highly
1274 vagile invasive species. *Molecular Ecology* [Internet] 30:1419–1434. Available from:
1275 <https://onlinelibrary.wiley.com/doi/abs/10.1111/mec.15601>
- 1276 Sutherst RW, Constable F, Finlay KJ, Harrington R, Luck J, Zalucki MP. 2011. Adapting to
1277 crop pest and pathogen risks under a changing climate. *WIREs Climate Change* 2:220–
1278 237.
- 1279 Suvorov A, Kim BY, Wang J, Armstrong EE, Peede D, D’Agostino ERR, Price DK, Waddell PJ,
1280 Lang M, Courtier-Orgogozo V, et al. 2022. Widespread introgression across a
1281 phylogeny of 155 *Drosophila* genomes. *Current Biology* [Internet] 32:111-123.e5.
1282 Available from: <https://www.sciencedirect.com/science/article/pii/S0960982221014962>
- 1283 Tepolt CK, Grosholz ED, de Rivera CE, Ruiz GM. 2022. Balanced polymorphism fuels rapid
1284 selection in an invasive crab despite high gene flow and low genetic diversity. *Molecular*
1285 *Ecology* [Internet] 31:55–69. Available from:
1286 <https://onlinelibrary.wiley.com/doi/abs/10.1111/mec.16143>
- 1287 Tepolt CK, Palumbi SR. 2020. Rapid Adaptation to Temperature via a Potential Genomic
1288 Island of Divergence in the Invasive Green Crab, *Carcinus maenas*. *Front. Ecol. Evol.*
1289 [Internet] 8. Available from:
1290 <https://www.frontiersin.org/articles/10.3389/fevo.2020.580701>
- 1291 Terhorst J, Kamm JA, Song YS. 2017. Robust and scalable inference of population history
1292 from hundreds of unphased whole-genomes. *Nat Genet* [Internet] 49:303–309.
1293 Available from: <https://www.ncbi.nlm.nih.gov/pmc/articles/PMC5470542/>
- 1294 Thompson MJ, Jiggins CD. 2014. Supergenes and their role in evolution. *Heredity* [Internet]
1295 113:1–8. Available from:
1296 <http://www.nature.com/hdy/journal/v113/n1/full/hdy201420a.html>
- 1297 Thornton T, Tang H, Hoffmann TJ, Ochs-Balcom HM, Caan BJ, Risch N. 2012. Estimating
1298 kinship in admixed populations. *Am J Hum Genet* 91:122–138.
- 1299 Timmeren SV, Isaacs R. 2014. *Drosophila suzukii* in Michigan vineyards, and the first report of
1300 *Zaprionus indianus* from this region. *Journal of Applied Entomology* 138:519–527.

- 1301 Uller T, Leimu R. 2011. Founder events predict changes in genetic diversity during human-
1302 mediated range expansions. *Global Change Biology* [Internet] 17:3478–3485. Available
1303 from: <https://onlinelibrary.wiley.com/doi/abs/10.1111/j.1365-2486.2011.02509.x>
- 1304 Vilela C. 1999. Is *Zaprionus indianus* Gupta, 1970 (Diptera, Drosophilidae) currently colonizing
1305 the Neotropical region? *Drosophila Information Service* 82:37–39.
- 1306 Weinig C, Brock MT, Dechaine JA, Welch SM. 2007. Resolving the genetic basis of
1307 invasiveness and predicting invasions. *Genetica* [Internet] 129:205–216. Available from:
1308 <https://doi.org/10.1007/s10709-006-9015-7>
- 1309 Wickham H. 2016. ggplot2: Elegant Graphics for Data Analysis.
- 1310 Willbrand B, Pfeiffer D, Leblanc L, Yassin A. 2018. First Report of African Fig Fly, *Zaprionus*
1311 *indianus* Gupta (Diptera: Drosophilidae), on the Island of Maui, Hawaii, USA, in 2017
1312 and Potential Impacts to the Hawaiian Entomofauna. *Proceedings of the Hawaiian*
1313 *Entomological Society* 50:55–65.
- 1314 Yassin A, Capy P, Madi-Ravazzi L, Ogereau D, David JR. 2008. DNA barcode discovers two
1315 cryptic species and two geographical radiations in the invasive drosophilid *Zaprionus*
1316 *indianus*. *Molecular Ecology Resources* [Internet] 8:491–501. Available from:
1317 <https://onlinelibrary.wiley.com/doi/abs/10.1111/j.1471-8286.2007.02020.x>
- 1318 Yassin A, David J. 2010. Revision of the Afrotropical species of *Zaprionus* (Diptera,
1319 Drosophilidae), with descriptions of two new species and notes on the internal
1320 reproductive structures and immature stages. *ZooKeys* 51:33–72.
- 1321 Zanuncio-Junior JS, Fornazier MJ, Andrezza F, Culik MP, Mendonça L de P, Oliveira EE,
1322 Martins D dos S, Fornazier ML, Costa H, Ventura JA. 2018. Spread of Two Invasive
1323 Flies (Diptera: Drosophilidae) Infesting Commercial Fruits in Southeastern Brazil. *flen*
1324 101:522–525.
- 1325 Zheng X, Levine D, Shen J, Gogarten SM, Laurie C, Weir BS. 2012. A high-performance
1326 computing toolset for relatedness and principal component analysis of SNP data.
1327 *Bioinformatics* 28:3326–3328.
- 1328